HHS Public Access

Author manuscript

Nat Cell Biol. Author manuscript; available in PMC 2014 January 01.

Published in final edited form as:

Nat Cell Biol. 2013 July ; 15(7): 773–785. doi:10.1038/ncb2791.

A Bcl-x_L-Drp1 complex regulates synaptic vesicle membrane dynamics during endocytosis

Hongmei Li[1], **Kambiz N. Alavian**[1], **Emma Lazrove**[1], **Nabil Mehta**[1], **Adrienne Jones**[1], **Ping Zhang**[1], **Pawel Licznerski**[2], **Morven Graham**[3], **Takuma Uo**[4], **Junhua Guo**[1], **Christoph Rahner**[3], **Ronald S. Duman**[2], **Richard S. Morrison**[4], and **Elizabeth A. Jonas**[1]

[1]Dept. Internal Medicine, Yale University, New Haven, CT, USA

[2]Dept. of Psychiatry, Yale University, New Haven, CT, USA

[3]Dept. Cell Biology, Yale University, New Haven, CT, USA

[4]Dept. of Neurological Surgery, U of Washington, Seattle, WA, USA

Abstract

Following exocytosis, the rate of recovery of neurotransmitter release is determined by vesicle retrieval from the plasma membrane and by recruitment of vesicles from reserve pools within the synapse, the latter of which is dependent on mitochondrial ATP. The Bcl-2 family protein Bcl-x_L, in addition to its role in cell death, regulates neurotransmitter release and recovery in part by increasing ATP availability from mitochondria. We now find, however, that, Bcl-x_L directly regulates endocytotic vesicle retrieval in hippocampal neurons through protein/protein interaction with components of the clathrin complex. Our evidence suggests that, during synaptic stimulation, Bcl-x_L translocates to clathrin-coated pits in a calmodulin-dependent manner and forms a complex of proteins with the GTPase Drp1, Mff and clathrin. Depletion of Drp1 produces misformed endocytotic vesicles. Mutagenesis studies suggest that formation of the Bcl-x_L-Drp1 complex is necessary for the enhanced rate of vesicle endocytosis produced by Bcl-x_L, thus providing a mechanism for presynaptic plasticity.

INTRODUCTION

BCL-2 family proteins participate in cell death [12-456, 7] but one member of the family, Bcl-x_L, is the predominant anti-apoptotic protein expressed in healthy adult brain [8] suggesting that it performs other physiological functions. In hippocampal neurons, over-expression of Bcl-x_L markedly changes synaptic morphology [9]. In the squid giant presynaptic terminal, recombinant BcL-x_L protein enhances the rate of recovery of neurotransmission following intense synaptic activity [10] while the Bcl-2/BcL-x_L inhibitor ABT-737 slows recovery [11].

Corresponding author: Elizabeth A Jonas Associate Professor Depts. Internal Medicine (Endocrinology) and Neurobiology Yale University School of Medicine PO Box 208020 New Haven, CT 06520 Elizabeth.jonas@yale.edu.

Bcl-x_L also regulates neuronal metabolism by enhancing the efficiency of mitochondrial ATP production[12]. Mobilization of synaptic vesicles from the reserve pool depends on mitochondria[13]. Following physiological exoctyosis, however, recovery of neurotransmitter pools is also determined by endocytotic retrieval of vesicles directly from the plasma membrane. The molecular machinery regulating retrieval includes the clathrin coat, which interacts with molecules that catalyze fission of synaptic vesicles from the plasma membrane[14, 15] and calcium dependent proteins and phosphatases which catalyze endocytosis[16, 17]. Both reserve pool mobilization and direct plasma membrane retrieval contribute to recovery in hippocampus[18].

We have now found using imaging techniques in hippocampal neurons that Bcl-x_L regulates recovery to a fast-releasing vesicle pool. Surprisingly, enhanced vesicle recovery produced by Bcl-x_L occurs even when effects of mitochondrial ATP are eliminated. Bcl-x_L-regulated recovery depends on stimulation, calmodulin and Bcl-x_L translocation to clathrin-coated pits. At synaptic vesicles, Bcl-x_L forms protein/protein interactions with the dynamin-like GTPase Drp1. Depletion of Drp1 or disruption of its interaction with Bcl-x_L slows endocytosis and produces aberrantly shaped vesicle membranes. We suggest that a Bcl-x_L-Drp1-clathrin complex directly enhances vesicle retrieval from the plasma membrane and contributes to enlargement of a fast-releasing pool during presynaptic plasticity.

RESULTS

Bcl-x_L over expression enhances the rate of release of styryl dyes in hippocampal neurons

To study the role of Bcl-x_L in vesicle exo- and endocytosis, we over-expressed GFP-Bcl-x_L or GFP control lentivirus constructs in cultured hippocampal neurons (DIV 14)[9] and measured the kinetics of release of the styryl dye FM-5-95 at individual synapses after loading with 47 mM KCl, 2 mM $CaCl_2$ for 90 s, a protocol reported to label recycling vesicles (Fig. 1a, Exp 1)[19-21]. Peak fluorescence of labeled presynaptic clusters and total change in fluorescence (ΔF) were significantly higher in Bcl-x_L over-expressing cells compared to controls (Fig. 1d and Supple. Fig. 1a) consistent with previous findings that Bcl-x_L increases presynaptic vesicle cluster size by light and electron microscopy [9]. Greater than 90% of dye was released within the first 90 s of stimulation in 90 mM KCl (Supple Fig. 1b), therefore only the first 90 s are shown in subsequent studies. In controls, release kinetics at room temperature were well fit with a single exponential (Fig. 1b, e, f); in all control experiments, fewer than 20% of puncta displayed bi-exponential kinetics of fluorescence decline. Relative weights of fits to rapid and slow components of release demonstrated that release in control cells had little or no rapid component (Fig. 1g). In contrast to controls, the kinetics of dye release in more than 90% of Bcl-x_L over-expressing neurons required a fit with two exponentials (Fig. 1b, e, f); the rapid component of release represented as much as one third or more of the total release (Fig. 1g). These data show that both controls and Bcl-x_L expressing cells have a slowly releasing pool, but that Bcl-x_L over-expressing cells have an additional pool that releases more rapidly.

Vesicle pool loading is regulated by calcium influx [20]. To determine if increased pool loading was related to calcium influx, calcium responses in GFP-Bcl-x_L and control GFP expressing cells were monitored with the calcium indicator fluo-4 during stimulation with

100 APs at 10 Hz. No difference in calcium levels at boutons between Bcl-x_L overexpressing cells and controls was detected (Fig. 1c), suggesting that differences in calcium influx at release sites do not contribute to differences in vesicle release.

In hippocampal neurons, filling of the fast-releasing pool takes longer than it does, for example, in the Calyx of Held[17, 22]; therefore refilling of the fast-releasing pool might take longer in controls compared to Bcl-x_L expressing cells. To test this, we allowed for continued dye loading after stimulation during a 5 minute re-filling period (Fig. 1a, Exp 2)[20]. Using this protocol Bcl-x_L over-expressing cells again demonstrated larger peak fluorescence than control neurons (Fig. 1h and Supple Fig. 1a), but kinetics of dye release from both Bcl-x_L and control neurons now required a fit with two exponentials (Fig. 1i-k). Therefore, like Bcl-x_L cells, control cells have a rapidly releasing pool, but this pool takes longer to fill than in Bcl-x_L cells.

The late-filling fast-releasing pool may continue to fill long after stimulation has ceased. If the fast-releasing pool fills faster in Bcl-x_L overexpressing cells, then there should exist a time after stimulation that the fast-releasing pool would be filled in the Bcl-x_L expressing cells but not in controls. To test if controls fill the fast-releasing pool long after stimulation, dye was presented for 90 s only at 3 minutes after the end of stimulation (Fig. 1a, Exp 3). In both controls and Bcl-x_L over-expressing cells, there was a lower level of peak fluorescence than in Exp 1 and 2 (Fig. 1l and Supple Fig. 1a), suggesting only partial filling of recovering pools; the filled pool sizes, however, of the two cell types were now not different from each other, therefore a large portion in Bcl-x_L over-expressing cells filled early. In addition, in Bcl-x_L cells, there was complete elimination of bi-exponential kinetics, suggesting Exp 3 eliminated filling of the fast-releasing pool (Fig. 1m-o). In controls however, release kinetics of some cells now required bi-exponential fits (Fig. 1n-o), suggesting very late re-filling of the fast-releasing pool.

Endogenous Bcl-x_L participates in normal vesicle pool dynamics

To determine if endogenous Bcl-x_L regulates normal exo-endocytosis we reduced levels of Bcl-x_L with Bcl-x_L shRNA or scrambled shRNA lentivirus and studied release properties of the recycling pool (Exp 1; Fig. 2a and Supple Fig. 1a). Cells expressing Bcl-x_L shRNA had decreased peak fluorescence compared to controls (Fig. 2b and Supple. Fig. 1a), confirming an effect on overall pool size[9]. Kinetics of the slowly releasing pool were decreased in Bcl-x_L depleted cells (Fig. 2c-e) suggesting that Bcl-x_L regulates the rate of exo-endocytosis of both the rapidly and slowly releasing pools.

Bcl-x_L acts downstream of calmodulin to enhance endocytosis

Re-filling of at least two vesicle pools in the Calyx of Held is dependent on calcium/calmodulin[23, 24], therefore inhibition of calmodulin could affect pool dynamics in hippocampal cells. Control neurons treated with the calmodulin inhibitor calmidazolium (CaMi, 20 μM for 30 min) during exo-endocytosis to the recycling pool manifested decreased peak fluorescence (Fig. 2f and Supple Fig. 1a) and a decreased time constant of release (Fig. 2g-i), suggesting that CaMi prevented re-filling of a slowly-releasing pool. If CaMi-sensitive pools were sensitive to Bcl-x_L, then Bcl-x_L over-expression might rescue

release kinetics in CaMi-exposed neurons. Consistent with this, CaMi treatment failed to decrease peak fluorescence in Bcl-x_L-over-expressing cells (Fig. 2j) and, although CaMi slowed bi-exponential kinetics (Fig. 2k, l), Bcl-x_L rescued the fast releasing pool in CaMi-treated cells (Fig. 2m). Therefore Bcl-x_L could act downstream of calmodulin in re-filling of vesicle pools.

Bcl-x_L increases rate of endocytosis in synaptopHluorin expressing neurons

Experiments on exo- and endocytosis using styryl dyes provide an indirect measure of the kinetics of endocytosis[25]. A direct measure is obtained using synaptopHluorin, a green fluorescent synaptic vesicle protein that increases its fluorescence upon exocytosis, when the lumen of synaptic vesicles is exposed to the relatively high pH of the external medium[26-29]. Upon endocytosis, fluorescence intensity declines, and the kinetics of decline reflect the rate of vesicle retrieval plus the rate of re-acidification of the vesicle lumen[29]. Using synaptopHluorin, Bcl-x_L overexpressing cells had higher peak fluorescence compared to controls during stimulation, as expected by the increased pool size (Fig. 3a). In addition, the time constant of the decrease in fluorescence following the end of stimulation was faster than in controls (Fig. 3a inset). Bcl-x_L over-expressing cells had an increase in peak fluorescence compared to control cells after addition of the vesicle re-acidification inhibitor bafilomycin (control data shown in Fig. 3b, d; Bcl-x_L over-expressing cell data shown in Fig. 3c, d) suggesting that Bcl-x_L over-expressing neurons perform more endocytosis during exocytosis compared to controls. In contrast, neurons expressing DsRed Bcl-x_L shRNA had slower fluorescence decline (Fig. 3e and inset) and a decrease in peak fluorescence in bafilomycin (controls shown in Fig. 3f, h; DsRed Bcl-x_L shRNA shown in 3g, h), indicating that Bcl-x_L is necessary for early pool loading during exocytosis. To control for off-target effects of shRNA, DsRed Bcl-x_L shRNA-expressing cells were transfected with an shRNA-resistant Bcl-x_L construct. This construct rescued the effects of Bcl-x_L depletion on protein level (Suppl. Fig. 2a, b) and synaptopHluorin fluorescence changes (Fig. 3i), confirming that the effect of Bcl-x_L shRNA was specific. The small molecule Bcl-x_L inhibitor ABT-737[11, 30] (Fig. 3j) also decreased the rate of decline in synaptopHluorin fluorescence after stimulation compared to that measured before ABT-737 exposure (Fig. 3j inset).

Reports have emphasized a role for Bcl-x_L in enhancing ATP availability for cell survival[31, 32]. If the sole effect of Bcl-x_L were to enhance ATP production by mitochondria the effects of Bcl-x_L on vesicle dynamics would be eliminated under conditions of fixed ATP such as in autaptically synapsing cells patch-clamped with ATP (1 mM) in the recording pipette (Fig. 3k; see methods). Under these conditions, synaptic depression was less in Bcl-x_L over-expressing cells than controls (Fig. 3l, m), suggesting that Bcl-x_L relieved synaptic depression, in part in an ATP-independent manner. To eliminate mitochondrial ATP production altogether, we exposed cells to the F_1F_O ATP synthase enzymatic inhibitor oligomycin. In the absence of oligomycin, as previously reported[12], overexpression of Bcl-x_L increased ATP levels over control neurons (Fig. 3n); 5 min. of exposure to oligomycin completely eliminated this difference (Fig 3n). Oligomycin also prolonged the time course of endocytosis more in controls than cells overexpressing Bcl-x_L (Fig. 3o, p). Nevertheless, the difference in ratio of peak fluorescence before and after bafilomycin exposure comparing Bcl-x_L expressing cells to controls (Fig. 3q-s) was

preserved in the presence of oligomycin (compare Fig. 3s to Fig. 3d). These data suggest that a portion of early endocytosis in Bcl-x_L-expressing neurons is unaffected by loss of mitochondrial ATP.

Neuronal stimulation promotes calmodulin-dependent Bcl-x_L translocation to synaptic vesicle membranes

During strong synaptic stimulation or injurious stimuli such as ischemia in neurons, large amounts of calcium enter the cell and are buffered by calcium buffering proteins, mitochondria and the endoplasmic reticulum. In cells that have received such stimuli, Bcl-x_L translocates to intracellular membranes perhaps to enhance synaptic responses and protect against cell injury[33-36]. To measure acute translocation of Bcl-x_L to intracellular membranes after stimulation, cells were immediately lysed and subjected to sub-cellular fractionation for Bcl-x_L immunoanalysis. The level of contamination of subcellular fractions with proteins specific to other fractions was low either before or after stimulation (Suppl. Fig. 2d) and the fraction containing synaptic vesicle protein (synaptotagmin-1) was relatively devoid of post-synaptic protein (PSD-95), presynaptic compartment or presynaptic membrane proteins (Suppl. Fig. 2e). Levels of endogenous Bcl-x_L after stimulation decreased in the cytosol and increased in mitochondria and in the synaptic vesicle membrane compartment (Fig. 4a, b). Bcl-x_L translocation was largely prevented by pre-teatment with CaMi (Fig. 4a, b), suggesting calmodulin is upstream of translocation. To rule out non-specific effects of calmodulin inhibition, neurons were depleted of endogenous calmodulin by shRNA (calmodulin protein blot Supple. Fig.2c). Translocation of Bcl-x_L was largely prevented in calmodulin depleted cultures (Fig. 4c, d), suggesting that calmodulin is necessary for Bcl-x_L translocation to both mitochondria and synaptic vesicle membranes during neuronal activity. Endogenous calmodulin also regulated early endocytosis, since neurons expressing calmodulin shRNA had a lower ratio of endocytosis to exocytosis measured with and without bafilomycin (Fig. 4e-g) and a slower rate of synaptopHluorin fluorescence decline (Fig. 4h and inset).

Bcl-x_L and Drp1 are co-localized with clathrin on synaptic vesicles and Drp1 regulates endocytotic vesicle morphology

Previous work suggested that Bcl-x_L co-localizes with and activates, via protein-protein interaction, the GTPase activity of Drp1 [9, 37]. Drp1 is a large dynamin-like GTPase usually associated with mitochondrial fission events in both physiological and pathological settings[9, 37-41]. We therefore determined if Drp1, in its role as a dynamin-like GTPase, might regulate endocytosis. Indeed, immuno-electron micrographs demonstrated that Drp1, although clearly localized in part to mitochondria (Suppl. Fig. 3a) was also co-localized with clathrin at clathrin-coated pits in neurons fixed just after stimulation (Fig. 5a) and translocated to synaptic vesicles in a stimulation-calmodulin dependent manner (Suppl. Fig. 3b). Furthermore, clathrin, Bcl-x_L and the Drp1 mitochondrial targeting protien Mff, but not dynamin or non-vesicular proteins (PSD-95 or Cacna1a) were present in immunoblots of brain tissue immunoprecipitated with anti-Drp1 antibody (Fig. 5b). The Bcl-x_L/Drp1/Mff/clathrin complex was also present in the purified synaptic vesicle fraction (Fig. 5c, d). The anti-Drp1 antibody was specific to Drp1 in that it did not recognize dynamin in brain

lysates; the anti-Dynamin I and II antibody was also specific in brain lysates (Suppl. Fig. 3c).

Bcl-x_L co-localizes with and activates the GTPase activity of Drp1 to alter membrane properties[9, 42]. To test if Drp1 influences normal exo-endocytosis, synaptopHluorin-expressing neurons were depleted of Drp1 by lentivirus encoding shRNA (Supple Fig. 2f); depletion of Drp1 was confirmed by immunoblots (Suppl. Fig. 2g, h) and in randomly generated immuno-electron micrographs of equal numbers of synaptic profiles (Suppl. Fig. 2i). We found previously that depletion of Drp1 or expression of a dominant negative defective Drp1 does not prevent mitochondrial entry into axons and dendrites, but increases the length of mitochondria in neuronal processes[9, 37, 43]. In the current study, Drp1 depletion increased individual mitochondrial area measured in electron micrographs (0.14 +/- 0.02 μ^2, N=18 mitochondria in controls compared to 0.30 +/- 0.03 μ^2, N=20 mitochondria in Drp1 shRNA, p = 0.0011), consistent with hyperfused mitochondria. Both peak fluorescence and rate of synaptopHluorin re-uptake in Drp1 depleted cells were decreased compared to scrambled shRNA controls (Fig. 5e) but Drp1 depletion was rescued by over-expression of an shRNA-resistant Drp1 construct, suggesting that Drp1 is specifically required for normal exo-endocytosis (Fig. 5f). Peak fluorescence ratio of bafilomycin-treated cells expressing Drp1 shRNA was decreased compared to controls (control data shown in Fig. 5g, i; Drp1 shRNA data shown in Fig. 5h, i), indicating that Drp1, like Bcl-x_L, is necessary for early vesicle re-uptake during exocytosis.

Drp1 is recruited to mitochondria via the mitochondrial fission factor Mff [44]. Mff coimmunoprecipitated with Drp1 in brain lysates, but also in purified synaptic vesicle lysates (Fig. 5b-d) and also co-immunoprecipitated with the specific vesicle membrane protein synaptotagmin (Fig. 5j). Depletion of Mff by shRNA produced a decline in the rate of endocytosis and a decrease in early endocytosis (Fig. 5k-m). Taken together, the findings suggest that Mff may serve as the targeting protein for Drp1 to synaptic vesicle membranes and that Mff contributes to vesicle retrieval from the plasma membrane after stimulation.

Bcl-x_L and Drp1-Mff previously were known to function at mitochondrial membranes, not synaptic vesicle membranes. Therefore, to confirm localization at synaptic vesicle membranes, immunogold electron microscopy was performed. Clathrin was co-localized with Bcl-x_L at clathrin-coated pits in control synapses (Fig. 6a). Bcl-x_L was present in brain tissue immunoprecipitated with anti-clathrin antibody (Fig. 6b), although synaptic proteins that are known not to bind clathrin (dynamin, Cacna1a and PSD-95) were absent, suggesting specific association of Bcl-x_L with clathrin. Formation of the Bcl-x_L-clathrin complex depended on neuronal stimulation: gold particles labeled with antibodies to clathrin and Bcl-x_L were increasingly co-localized after stimulation (N=27) compared to non-stimulated synapses (N=25; Fig. 6c).

Bcl-x_L and Drp1 were found to be localized to mitochondria, but also at synaptic vesicle membranes with the presynaptic vesicle marker synaptophysin (Fig. 6d, f). Labeling with synaptophysin was specific because it was restricted to synaptic vesicle membranes. Labeling of Bcl-x_L and Drp1 was specific, because it was restricted to synaptic vesicle membranes and to mitochondria but little labeling was seen at other subcellular locations

including post synaptic sites (Fig. 6d, f). Bcl-x_L and Drp1 co-localized with synaptic vesicle components in a stimulation dependent manner; both Bcl-x_L and Drp1 were increased in synaptic profiles after stimulation and co-localization with synaptophysin was increased (Fig.6 e).

A morphologically apparent defect in endocytosis occurred in Drp1 depleted resting cultured neurons (Fig. 7a-c). Images of scrambled shRNA-expressing synapses only occasionally displayed enlarged endosomal or vesicular structures (Fig. 7a) whereas images of Drp1 shRNA-expressing synapses showed multiple large vesicular structures (Fig. 7b). In addition, measurable synaptic vesicle area in electron micrographs of Drp1-depleted synapses was more variable and contained larger vesicles than controls (Fig. 7c). It is likely that enlarged structures represent either vesicles delayed in the process of endocytosis, enlarged as a result of abnormally flat membrane curvature or abnormally fused with partner vesicles.

Electron micrographs of stimulated HRP-labeled synapses demonstrated a similar bizarre endosomal phenotype as seen in non-stimulated neurons, and this phenotype was rarely present in controls (Fig. 7d). As was the case for non-stimulated synapses, the average area of HRP-labeled vesicles was significantly larger in Drp1-depleted cells compared to controls (Fig. 7e). The large endosomal structures in stimulated Drp1 depleted neurons co-localized with the specific synaptic vesicle protein VAMP on immuno-electron micrographs (Fig. 7f and i), suggesting they had the phenotype of synaptic vesicles. In addition, unlike in controls, where large endosomal structures were observed rarely before stimulation (Fig. 7g top and quantification in 7h), after Drp1 depletion, abnormal vesicular profiles including long tubular and enlarged endosomal/vesicular structures were present almost equally in stimulated and resting cells (Fig. 7g bottom and quantification in 7i), suggesting that abnormal structures may be delayed in devolving into normal vesicles.

In normal neurons undergoing stimulation, the plasma membrane perimeter (synapse profile area) may increase as exocytotic membrane is added to it; concomitantly the number of intra-synaptic vesicles is decreased after fusion[45]. We found in control neurons that the area of synaptic profiles was not changed after stimulation, but that the number of synaptic vesicles was decreased (Fig. 7j, k). In contrast, in Drp1-depleted cells, the number of synaptic vesicles was unchanged after stimulation but synaptic profile area was decreased, perhaps consistent with re-uptake of enlarged membranes and lack of re-formation of vesicles (Fig. 7j, k). Interestingly, synaptic profile area and number of vesicles in unstimulated Drp1-depleted synapses were significantly decreased compared to unstimulated controls, consistent with the notion that Drp1-depleted synapses are unable to maintain normal vesicle pool sizes.

Bcl-x_L/Drp1 interaction is required for regulation of endocytosis

To confirm the role in endocytosis of the Bcl-x_L/Drp1 complex, mutations in Bcl-x_L were designed *de novo.* We mutated conserved amino acids between human Bcl-x_L and Bcl-2-like protein CED-9 of *Caenorhabditis elegans*, since both proteins interact with Drp1 [9, 46]. Mutation of three consecutive conserved amino acid residues in the BH1 domain and three conserved residues in the BH2 domain generated constructs M1 and M2 (Fig. 8a).

Immunoprecipitation by anti-FLAG antibody of wild type and M1 FLAG-tagged Bcl-x_L proteins pulled down over-expressed Drp1 in HEK293T cells, while FLAG-tagged M2 Bcl-x_L protein failed to interact with over-expressed Drp1 (Fig. 8b). Over-expression of wild type Bcl-x_L and M1 equally enhanced synaptopHluorin responses in hippocampal neurons, but over-expression of M2 failed to enhance responses over the control level (Fig. 8c, d). The synaptopHluorin experiments and analyses were performed by an operator blinded to the results of the co-immunoprecipitation studies. The Bcl-x_L/Drp1 complex therefore enhances endocytosis through a mechanism involving direct interaction between the two proteins (Fig. 8e).

DISCUSSION

We suggest that Bcl-x_L, previously known to protect against cell death, also regulates vesicle endocytosis in hippocampal neurons. We show that Bcl-x_L interacts in a complex with clathrin and Drp1 to alter the kinetics of vesicle pool recovery.

We have previously shown in squid that Bcl-x_L protein enhances recovery to a rapidly releasing neurotransmitter pool following synaptic depression[10] and that endogenous Bcl-x_L regulates this recovery[11]. Although at least two pools regulate vesicle recovery at the Calyx of Held and squid, hippocampal presynaptic terminals do not display the same fast time kinetics as these synapses[10, 47]. Although previous work in other synapses suggested that transmitter recovery was regulated by mitochondria[10], we find a pool in hippocampus that is resistant to mitochondrial metabolism. Nevertheless, it is likely that other synaptic processes in hippocampus are dependent on mitochondrial function[9, 48].

Release kinetics in the hippocampus are determined by calcium-dependent synaptic vesicle priming, fusion, and recycling. In support of a role for calcium-dependent processes, we find that inhibition of calmodulin by pharmacological or genetic means prevents Bcl-x_L and Drp1 translocation to synaptic vesicles during stimulation and prevents normal vesicle pool recovery. In this form of clathrin-dependent endocytosis, we find that Bcl-x_L and Drp1 act downstream of calcium influx/calmodulin. Our studies are also consistent with recent results defining a role for calmodulin in vesicle release probability[49]. Indeed, our electron micrographs of Drp1-depleted cells demonstrate a lack of change in vesicle number after stimulation, suggesting defective exocytosis.

Previous studies support a role for BCL-2 family proteins including Bcl-x_L in altering lipid membrane morphology in cell-free systems[50-53]. Bcl-x_L may change membrane morphology through its actions on Drp1. GTPases participate in membrane fission events of several subcellular organelles. Drp1 acts downstream of Bcl-x_L [9, 37] and upstream of endophilin B1 in regulating mitochondrial membrane remodeling[54]. Endophilin family members also play a role in synaptic endocytosis[55-58]. The GTPases at vesicles interact with AP2, epsin, amphiphysin and AP180 [15, 59] to alter membrane curvature and achieve scission of the vesicle from the plasma membrane. We find that interaction of Bcl-x_L with Drp1 is necessary for normal vesicle retrieval; a mutation in the Bcl-x_L BH2 domain decreases interaction with Drp1 and inhibits Bcl-x_L-induced increase in endocytosis rate. We find that the mitochondrial docking protein Mff[44] also recruits Drp1 to synaptic vesicles. However,

the mechanism by which Mff recruits Drp1 to synaptic vesicles vs. mitochondria is not known.

Drp1 has been implicated previously, albeit indirectly, in the regulation of synaptic vesicle endocytosis. In *Drosophila* synapses, Drp1 knockout produces loss of mitochondrial targeting to synapses and a metabolically dependent decline in sustained synaptic responses[13, 60]. Previous work also supports a role for Drp1 in hippocampal synapse formation and enlargement. Expression of a dominant negative form of Drp1 decreases mitochondrial targeting to synapses and decreases synapse formation even though it lengthens mitochondria in neuronal processes[9]. Nevertheless, a direct role for Drp1 at synaptic vesicle membranes has not been anticipated previously. Our current study shows that Drp1 depletion enlarges endocytotic figures creating abnormally flat membrane curvature, associated with delayed vesicle recovery to release ready pools. Based on our findings the order of events in healthy synapses undergoing exo/endocytosis would be 1) calcium entry into the terminal, 2) activation of calmodulin, 3) translocation of Bcl-x_L/Drp1 to the synaptic vesicle membrane, 4) binding of Bcl-x_L/Drp1 to a complex including Mff and clathrin, 5) enhancement of the rate of retrieved membrane to re-form into exocytosis-ready vesicles (Fig. 8e). It is tempting to speculate based on these data that a complex of proteins involving Bcl-x_L, Drp1 and clathrin, in cooperation with other known vesicle membrane-regulating proteins, is necessary for efficient endocytosis and presynaptic plasticity.

EXPERIMENTAL PROCEDURES

Primary cultures of rat hippocampal neurons and transfections

Primary rat hippocampal neurons were prepared as described previously [61, 62]. Briefly, hippocampi were isolated from Sprague-Dawley rat embryos (E18–E19), and then incubated for 12 min with 0.03% trypsin. The hippocampal cells were dissociated by trituration through a polished Pasteur pipette. Neurons were plated on 0.1% (w/v) poly-L-lysine (Peptides International, Louisville, KY) coated coverslips (Warner Instruments, Hamden, CT) at a density of 3–6 $\times 10^3$ cm^{-1}. Cells were cultured in Neurobasal medium, supplemented with B-27 (Invitrogen, Carlsbad, CA), 0.5mM glutamine, 25 μM glutamate, and 5% fetal calf serum. 3-4 hr after plating, the medium was replaced with serum-free Neurobasal supplemented with B-27 and 0.5mM glutamine. Cultures typically contained few glial cells, started to form synapses after 6 days *in vitro*, and were used 9 to 20 days after plating. Neurons were transfected with 2.5 M calcium phosphate at day 5 after plating with an efficiency of ~1 - 5%. Neurons were transduced with the lentiviral construct for Bcl-x_L at DIV 4-7 days and studied at DIV 12-18 with an efficiency of near 100%.

Viral constructs

Lentiviruses expressing Bcl-x_L with an N-terminal GFP tag were used to transduce cultured hippocampal neurons. Full length GFP- Bcl-x_L was subcloned into a lentivirus vector c-FUW [63]. Viral constructs were packaged in 293T cells by co-transfection with packaging plasmid delta 8.9 and envelope plasmid VSVG.48. 60h after transfection, virus-containing

supernatant was collected, stored at −80°C, and used for transduction of cultured hippocampal neurons on DIV-5.

Autaptic primary hippocampal neuron culture

Briefly, the center of each coverslip was treated with a 0.15% type IIA agarose solution and coverslips were dried for 1 h [64]. Micro-islands were prepared 2 days before plating hippocampal neurons. by spraying coverslips with 1:4 vol./vol. mixture of collagen and poly-D-lysine using a Glass micro-atomizer (Thomas Scientific, Swedesboro, NJ, USA). After drying, the coverslips were UV sterilized for 5 min. then pre-incubated for 1 h with neurobasal (+B27) medium + 10%FBS before plating with dissociated hippocampal cells at a density of $0.2–0.6\times10^4$ cells/ml. Island cultures were maintained for upwards of 6 weeks, typically cells were recorded at DIV 30.

Lentiviral shRNA knockdown of Bcl-x_L, Mff, Calmodulin and Drp-1 and the shRNA-resistant constructs

The lentiviral plasmids, expressing short hairpin RNAs (shRNA) were from Open Biosystems, USA. Lentiviral plasmids for Drp1 shRNA were designed as in [45]. The hairpin sequence against rat Bcl-x_L was: CGGGCTCACTCTTCAGTCGGAATAGTGAAGCCACAGATGTATTCCGACTGAAGAGTGAGCCCA For control, the scrambled, nonsilencing shRNA sequence (Open Biosystems catalog no. RHS4346) was used. The lentivirus was produced according to published methods [61]. The pGIPZ vectors, containing either shRNA sequence against Bcl-x_L or the scrambled sequence were co-transfected with the packaging Δ8.9 and the vesicular stomatitis virus G protein vectors into HEK 293T cells. 48 hours after transfection, the supernatant was centrifuged at 50,000×g. The viral pellet was resuspended in PBS and added to the hippocampal neuronal cultures DIV 5-7 and studied DIV 12-14. For the ds-RED constructs, the shRNA sequences targeting rat Bcl-x_L, Calmodulin1+2 and Drp1 were cloned through a shuttle vector pCMV-U6 into a modified version of the lentiviral expression vector FlkURW (1) creating FU6siGURW (includes the U6 promoter in front of the Ubiquitin promoter/dsRED2 expression cassette). The structure of the shRNA hairpins was sense-loop-antisense. The shRNA sequences were:

Bcl-x_L up:
TTTggagtcagtttagcgatgtcgGTGAAGCCACAGATGcgacatcgctaaactgactccTTTTT

Bcl-x_L down:
CGAAAAAggagtcagtttagcgatgtcgCATCTGTGGCTTCACcgacatcgctaaactgactc

Calm 1+2 up:
TTTgaagctttctccctatttgaGTGAAGCCACAGATGtcaaatagggagaaagcttcTTTTT

Calm 1+2 down:
CGAAAAAgaagctttctccctatttgaCATCTGTGGCTTCACtcaaatagggagaaagctt

Drp1 up:
TTTgacatcatccagctgcctcagGTGAAGCCACAGATGctgaggcagctggatgatgtcTTTTT

Drp1 down:
CGAAAAAgacatcatccagctgcctcagCATCTGTGGCTTCACctgaggcagctggatgatgt

The shRNA sequence against Mff was: 5'-**GATCGTGGTTACAGGAAATAA-3'.**

The Bcl-x_L and Drp1 shRNA-resistant constructs were made using the QuikChange Site-Directed Mutagenesis Kit (Agilent Technologies, USA) according to the manufacturer's protocol. Five and six silent mutations were placed, respectively, in the coding sequences of Bcl-x_L and Drp1, cloned in Flag and HA tag vectors. The sense sequences for the mutagenesis primers were: 5'-cccagaaaggatacagctggagCcaAttCagCgaCgtggaagagaacaggactgagg-3' for Bcl-x_L and 5'-caacacggtgggcgccgacGtcGtcTagTtgTctTaaatcgtcgtagtgggaac-3' for Drp1.

Design of Bcl-x_L mutants and Bcl-x_L – Drp1 Interaction by co-immunoprecipitation

In order to identify the specific Drp1-interacting domains on Bcl-x_L, BLAST analysis was performed to identify the conserved amino acids between human Bcl-x_L and CED-9 protein sequences. Two mutant constructs were produced each carrying three substitutions for completely conserved amino acids on the BH1 or BH2 domains of Bcl-x_L using the QuikChange Site-Directed Mutagenesis Kit (Agilent Technologies, USA) and the following primers: M1 5'-gtcgcattgtggccttttctactgctgcggggcactg-3'; 5'-cagtgccccgcagcagtagaaaaaggccacaatgcgac-3' M2 5'-ccaggagaacggcggctcggttacttgtgtggaactctatgg-3'; 5'-ccatagagttccacacaagtaaccgagccgccgttctcctgg-3'. The resulting mutations were: (M1: S145Y, F146C, G147C) (M2: W188S, D189V, F191C) (Fig. 7A). The constructs were expressed in 293T cells and immunoprecipitated, using the EZview^™ Red ANTI-FLAG^® M2 Affinity Gel (Sigma, USA), according to the manufacturer's protocol. The IP samples were examined by Western blot analysis using a rabbit anti-Bcl-x_L (Cell Signaling Technology) and a rabbit anti-Drp1 antibody (Santa Cruz Biotechnology)(for details see immunoblot section of methods).

Fluorescent measurement of pre-synaptic activity, using SynaptopHluorin

Neurons were co-transfected with RFP-Bcl-x_L or mito-RFP and SynaptopHluorin constructs using 2.5M calcium phosphate on DIV-5. Transfection efficiency was about 1–5%. The SynaptopHluorin-expressing neurons were assayed on DIV 14-18. The coverslips were mounted in the field stimulation chamber (platinum bath electrodes) on the stage of a microscope. The 50μl chamber was perfused at a rate of 2 ml/min at room temperature with saline solution containing in mM: 119 NaCl, 2.5 KCl, 2 CaCl2, 2 MgCl2, 25 HEPES, 30 glucose (buffered to pH 7.4, 300 mOsm). 10uM CNQX, 50uM AP5 (Sigma, USA) were added into the solution to prevent recurrent activity. Neurons were stimulated at 10Hz (50 mA, 1 ms pulses) for 20s. After 5 min at rest neurons were stimulated again at 10Hz for 20s in the presence of 5μM bafilomycin A1 (Calbiochem/ EMD Biosciences, CA). Fluorescence values for baseline were obtained by averaging 3 images at rest before the stimulus. Time course of fluorescence responses of sPH were measured from time-lapse images taken every 3 seconds. Quantitative measurements of fluorescence intensity at individual boutons were obtained by averaging 4×4 area pixels (0.4 × 0.4 um^2) corresponding to the center of

individual puncta, selected by hand, background subtracted, and processed using Axiovision Measurement Suite.

Fluorescent measurement of pre-synaptic activity, using FM5-95 dye

FM5-95 dye (Molecular Probes) was used at a final concentration of 30μM. 10μM CNQX and 50μM AP5 (Sigma, USA) were added into Tyrode's solution to prevent recurrent activity. Experiments were done in pairs of control and Bcl-x_L over-expressing neurons. All experiments were performed at room temperature.

1.Recycling pool loading protocol—FM5-95 dye was added to 47mM high K Tyrode's solution (47mM KCl, 107mM NaCl, 2mM $MgCl_2$, 10mM glucose, 10mM HEPES, 2mM CaCl2 (pH 7.4, 300 mOsm)) and put on cultured rat hippocampal cells. Neurons were given 90s to load the dye, after which it was washed out with perfusion (2.5ml/min) of a modified Tyrode's wash solution (no-Ca^{2+}) containing 150mM NaCl, 4mM KCl, 2mM MgCl2, 10mM glucose, 10mM HEPES (pH 7.4, 300mOsm). Wash was performed for 2 min. 90 images were taken with a 1 second interval between each while cells were being stimulated with 90mM KCl in Tyrode's solution (90mM KCl, 64mM NaCl, 2mM $MgCl_2$, 10mM glucose, 10mM HEPES, 2mM $CaCl_2$ (pH 7.4, 300mOsm).

2. Extended Load time protocol—FM5-95 dye was added to 47mM K+ Tyrode's solution for 90s. The High KCl-containing solution was washed out (2.5 ml/min) with modified Tyrode's wash solution containing FM 5-95 for 5min. Then, the dye was washed out by modified Tyrode's wash solution (2 min, 2.5 ml/min) lacking FM5-95 for 2 min. Cells were stimulated with 90mM high K^+ Tyrode's solution for 90s, while images were taken with a 1 second interval between each image.

3. Delayed labeling protocol—Cells were stimulated with 47mM KCl for 90s without FM5-95 dye, followed by a constant wash (2 min, 2.5ml/min) for 2-4 min. FM5-95 dye was then added to the wash for 90s followed by a wash (2 min, 2.5ml/min). Cells were then stimulated with 90mM high K Tyrode's solution while 90 images were taken with a 1 second interval between each image.

Image Analysis

Images were analyzed using Axiovision LE software and Microsoft Excel. The fluorescence signal of each SV punctum (4× 4 area pixels) was outlined and measured for all 90 images. A background measurement for each image was subtracted from the measurement of each punctum.

Calcium measurement

Neurons were loaded with 5μM fluo-4AM calcium indicator (Molecular Probes: F14201) and incubated at 37°C for 30min in dark. Fluorescent axonal varicosities correspond to synaptic boutons along hippocampal cell axons detected in phase images of the cultured neurons according to the methods of [65].

Fluorescence values for baseline were obtained by averaging 3 images at rest before the stimulus. Cells were stimulated with 100 stimuli (50mA, 1ms) at10Hz. Time course of fluorescence responses of dye were measured from time-lapse images, taken every 3 seconds. 5 regions of interest (ROI's) were selected per image and the average background value was subtracted from the signal value from each pixel in the field. Axiovision-4 software was used to collect time-lapse measurements. Quantitative measurements of fluorescence intensity of individual puncta were obtained by averaging 4×4 pixels (0.4 × 0.4um2). Experiments were done in pairs of control and Bcl-xL overexpressing neurons at 14DIV.

Immunoprecipitation and Western Blot analysis

Lysates of hippocampal cultures (DIV12) or adult whole brain were prepared with cell lysis buffer (10mM Hepes, 1mM EDTA (pH 7.4), 150mM NaCl, 1% Triton X-100, supplemented with protease inhibitors (Roche Applied Science)) for immunoprecipitation (IP) and Western blotting. Input represents 5% of total lysate. For translocation of endogenous Bcl-x_L, all cultures over-express GFP-Bcl-x_L but the bands shown are those of endogenous Bcl-x_L. All lanes contain 10 μg protein. For IP, cell lysate was mixed with primary antibody (1:1,000 dilution) in IP buffer (10mM Hepes, 1mM EDTA (pH 7.4), 150mM NaCl, 1% Triton X-100, supplemented with protease inhibitors) and incubated overnight at 4°C with gentle rocking. Protein A and G-Sepharose beads were added and allowed to incubate for 1 h. The unbound protein was removed by washing the beads three times in IP buffer. The bound protein was then eluted from the beads with SDS/PAGE sample buffer. Immunoprecipitated samples were analyzed by Western blotting, using previously published protocols (Li et al. 2008).

Western blot quantification

The quantification of protein levels was done using (http://rsb.info.nih.gov/ij/). Each band was normalized against its own internal control (lower bands). The values from independent experiments were then normalized against the mean of the group.

Antibodies used for immunoblotting analysis

Rabbit anti-human Bcl-x_L (1:1000; A. G. Scientific) or rabbit mAb anti-Bcl-x_L antibody 54H6 (1:1000; Cell Signaling Technology) or Anti-Bcl-x_L &s (BIOCARTA**),** Rabbit polyclonal anti-Drp1 (H-300; sc-32898, 1:1000; Santa Cruz Biotechnology), Mouse Anti-Synaptotagmin1/2 Monoclonal Antibody, Unconjugated, Clone 1D12 **(**MBL International). Dynamin I/II Antibody (#2342 1:1000 Cell Signaling Technology), GAPDH (6C5) (sc-32233 1:1000 ; Santa Cruz Biotechnology), COX-IV antibody [20E8] -Mitochondrial Loading Control (ab14744, 1:1000 abcam), Clathrin LCA (H-55): sc-28276, 1:1000; Santa Cruz Biotechnology), rabbit polyclonal antibody P/Q-type Ca++ CP α1A (H-90): sc-28619 from SANTA CRUZ BIOTECHNOLOGY, INC.(1:800), rabbit polyclonal antibody PSD95 from cell signaling (1:1000), Bassoon (D63B6) Rabbit mAb from cell signaling (1:1000); rabbit polyclonal anti-VDAC antibody (Cell signaling #4866, 1:1000); mouse monoclonal anti-synaptophysin antibody (Millipore MAB368, 1:20 for EM); polyclonal rabbit anti-Mff

antibody (Sigma HPA010968; 1:200); polyclonal rabbit anti-VAMP2 antibody (Synaptic Systems Cat No. 104 202; 1:20 for EM).

Sample Fixation for ImmunoElectron microscopy

Samples were fixed in 4% paraformaldehyde in 0.25M Hepes for 1 hour. Samples were rinsed in PBS and re-suspended in 10% gelatin, chilled and trimmed to smaller blocks and placed in cryoprotectant of 2.3M sucrose overnight on a rotor at 4C. They were transferred to aluminum pins and frozen rapidly in liquid nitrogen. The frozen block was trimmed on a Leica Cryo-EMUC6 UltraCut and 65-75nm thick sections were collected using the Tokoyasu method [66]. The frozen sections were collected on a drop of sucrose, thawed and placed on a nickel formvar /carbon coated grid and floated in a dish of PBS ready for immunolabeling.

Immunolabeling of sections

Grids were placed section side down on drops of 0.1M ammonium chloride to quench untreated aldehyde groups, then blocked for nonspecific binding on 1% fish skin gelatin in PBS. Single labeled grids were incubated on either a primary antibody rabbit anti-Bcl-X (Biocarta) 1:50, mouse anti-Clathrin (Chemicon) 1:75 dilutions for 30mins, or DRP1 (H-300): sc-32898 (1:50) from Santa Cruz Biotechnology, Inc. A rabbit anti mouse bridging antibody (Jackson) was used for the mouse primaries before rinsing and using 10nm protein A gold (UtrectUMC) for 30minutes. Double labeled grids used the primary rabbit anti-Bcl-X and 10nm protein A gold followed by rabbit anti-mouse bridge and the 5nm protein A gold. All grids were rinsed in PBS, fixed using 1% gluteraldehyde for 5mins, rinsed and transferred to a UA/methylcellulose drop, then dried for viewing. Samples were viewed FEI Tencai Biotwin TEM at 80Kv. Images were taken using Morada CCD and iTEM (Olympus) software.

Sample fixation for regular epon embedding (for studies with Drp1 shRNA)

Cells on coverslips were fixed in 2.5% gluteraldehyde in 0.1M sodium cacodylate buffer pH7.4 with for 1 hour. The samples were rinsed in sodium cacodylate postfixed in 1% osmium tetroxide for 1 hour, en bloc stained in 2% uranyl acetate in maleate buffer pH5.2 for a further hour then rinsed, dehydrated in an ethanol series and infiltrated with resin (Embed812 EMS). Resin filled gelatin capsules were inverted over the coverslip and baked overnight at 60°C. 60nm sections were cut using a Leica UltraCut UCT, collected on nickel formvar/carbon coated grids, stained using 2% uranyl acetate and lead citrate.

Protocol for HRP-staining neurons-Labeling endocytic vesicles with HRP

Neurons were rinsed with Tyrodes buffer and incubated with 10mg/ml HRP at 37°C for 20min. Cells were then stimulated with 90mM KCL for 90s following by 2X rinsing with ice cold Tyrodes buffer. Neurons were fixed for 1h with 1.2% glutaraldehyde and 0.1M NaCacodylate and incubated for 10min in 0.1M ammonium phosphate pH7.4. Neurons were incubated for another 10min in ammonium phosphate pH7.4. plus 0.5mg/ml diaminobenzidine(DAB) followed by incubation in 0.1M ammonium phosphate pH7.4, 0.5mg/ml DAB and 0.005% H_2O_2 for 5-15min (until brown color developed). Cells were

rinsed 3X with cold water and fixed for 1h in 1%OsO_4, 1%$K_4Fe(CN)_6$ and 0.1M Na Cacodylate, following with 3X5min washes with 0.1M NaCacodylate and 3x5min washes with water. Cells were stained overnight with 0.5% Uranyl magnesium acetate (2μm filtered) and washed 3x5min with water, 2x5min with 70% EtoH, 2x15min with 95% EtoH, 2x30min with 100% EtoH, 1 hr with 1:1 Epon-EtOH and 2x1hr with Epon. Cells were then embedded and baked for 48hr at 65°C.

Subcellular fractionation

Mitochondrial, synaptosomal and cytosolic fractions were prepared according to the manufacturers protocol (Millipore Cat. No. MIT1000). Briefly, cultured neurons were homogenized in isotonic Mitochondrial Buffer and centrifuged at 600xg for 10min at 4°C. The pellet, containing the nuclear and unbroken cells was discarded and the supernatant, containing the mitochondrial, synaptosomal and cytosolic fractions was centrifuged at 10,000xg for 30min at 4°C. The supernatant, containing the cytosolic fraction was separated from the pellet. The pellet containing the mitochondrial and synaptosomal fractions was resuspended in 100μL isolation buffer and layered onto a 7.5-10% Ficoll gradient. After 30min ultracentrifugation at 90,000xg, 4°C, the mitochondrial pellet and the middle layer, containing synaptosomes were removed and resuspended in isolation buffer and centrifuged for 10 min at 20,000xg, resulting in a crude synaptosomal pellet. Synaptosomal pellet was lysed by hypoosmotic shock in water. The samples were agitated for 30min in 4mM Hepes at 4°C, synaptosomal pellet was centrifuged for 20min at 25,000×g, resulting in a synaptosomal membrane fraction (pellet) and a synaptic vesicle fraction. The latter was used for immunoblots.

Electrophysiology

Whole-cell patch-clamp recordings were performed on autaptic hippocampal neurons in culture. Data were acquired using a EPC8 amplifier and Clampex 9.0 software. Recordings were filtered at 1 kHz and sampled at 2 ms. The bath solution contained the following (in mM): 124 NaCl, 3 KCl, 10 HEPES, 5 D-glucose, 2 CaCl2, 1 MgCl2, pH7.3, 275 mOsm. The pipette internal solution contained the following (in mM): 120 K-gluconate, 8 NaCl, 0.5 EGTA, 10 HEPES, 1 Mg-ATP, 10 QX-314. pH7.3. 265 mOsm. Stimulation was applied by depolarizing the cell via the recording electrode with the following membrane potential steps: −60mV, 20mV and −60mV, at 10 Hz. Synaptic current responses to depolarization were recorded at −60mV. Such currents were eliminated in the presence of CNQX/APV (data not shown). Series resistance ranged between 6-20 MΩ.

Luciferase assay for *in vitro* ATP measurements

Cellular ATP levels were measured upon acute cell membrane lysis of hippocampal neurons in a plate reader (Perkin-Elmer) in the presence of Luciferin/luciferase (ApoSENSOR, Biovision, Mountain View, CA).

Antibodies used in studies

Rabbit mAb anti-Bcl-xL antibody 54H6 (#2764, Cell Signaling Technology, 1:1000;), Rabbit Anti- Bcl-xL &s (#IMG 276, BIOCARTA), Rabbit anti-human Bcl-xL (#B1225, A.

G. Scientific,1:1000;), Rabbit anti-Drp1 (sc-32898, Santa Cruz 1:1000), Mouse Anti-Synaptotagmin1/2 Monoclonal Antibody, Unconjugated, Clone 1D12 (#D156-3, MBL International, 1:1000), Dynamin I/II Antibody (#2342 ,1:1000 Cell Signaling Technology), mouse anti-GAPDH (6C5) (sc-32233 ,1:1000 ; Santa Cruz Biotechnology), COX-IV antibody [20E8] -Mitochondrial Loading Control (ab14744, 1:1000 , abcam), Clathrin LCA (H-55): (sc-28276, 1:1000; Santa Cruz Biotechnology), Rabbit polyclonal antibody P/Q-type Ca++ CP 1A (H-90): sc-28619 Santa Cruz Biotechnology 1:800, Rabbit polyclonal antibody PSD95 (#2507, cell signaling ,1:1000), Rabbit mAb Bassoon (D63B6) (#6897, cell signaling ,1:1000), Rabbit anti-VDAC (#4866, Cell Signaling, 1:1000), mouse monoclonal anti-synaptophysin antibody (clone SVP-38, #MAB368, 1:20 for EM, Millipore), polyclonal rabbit anti-Mff antibody (HPA010968; Sigma ,1:200), polyclonal rabbit anti-VAMP2 antibody (#104202; 1:20 for EM Synaptic Systems).

Statistical Methods

Statistical analysis. For comparisons involving two groups, paired or unpaired Student's t -tests (two-tailed) were used. In all figures, *=P < 0:05, **= P < 0:01 and ***=P <0:001 denote significance level, and exact P values are provided in the figure legends.

Supplementary Material

Refer to Web version on PubMed Central for supplementary material.

ACKNOWLEDGMENTS

The authors wish to acknowledge Len Kaczmarek for thoughtful discussions of the data. The authors also thank Dr. Gero Meisenbock for providing Synapto-pHluorin for the sPH studies.

REFERENCES

1. Adams JM, Cory S. The Bcl-2 apoptotic switch in cancer development and therapy. Oncogene. 2007; 26:1324–1337. [PubMed: 17322918]
2. Banasiak KJ, Xia Y, Haddad GG. Mechanisms underlying hypoxia-induced neuronal apoptosis. Prog Neurobiol. 2000; 62:215–249. [PubMed: 10840148]
3. Youle RJ, Strasser A. The BCL-2 protein family: opposing activities that mediate cell death. Nat Rev Mol Cell Biol. 2008; 9:47–59. [PubMed: 18097445]
4. Fannjiang Y, et al. BAK alters neuronal excitability and can switch from anti- to pro-death function during postnatal development. Developmental cell. 2003; 4:575–585. [PubMed: 12689595]
5. Kim H, et al. Hierarchical regulation of mitochondrion-dependent apoptosis by BCL-2 subfamilies. Nat Cell Biol. 2006; 8:1348–1358. see comment. [PubMed: 17115033]
6. Wang C, Youle RJ. The role of mitochondria in apoptosis*. Annu Rev Genet. 2009; 43:95–118.
7. Hardwick JM, Youle RJ. SnapShot: BCL-2 proteins. Cell. 138:404. [PubMed: 19632186]
8. Krajewska M, et al. Dynamics of expression of apoptosis-regulatory proteins Bid, Bcl-2, Bcl-X, Bax and Bak during development of murine nervous system. Cell Death Differ. 2002; 9:145–157. [PubMed: 11840165]
9. Li H, et al. Bcl-xL induces Drp1-dependent synapse formation in cultured hippocampal neurons. Proc Natl Acad Sci U S A. 2008; 105:2169–2174. [PubMed: 18250306]
10. Jonas EA, et al. Modulation of synaptic transmission by the BCL-2 family protein BCL-xL. J Neurosci. 2003; 23:8423–8431. [PubMed: 12968005]

11. Hickman JA, Hardwick JM, Kaczmarek LK, Jonas EA. Bcl-xL inhibitor ABT-737 reveals a dual role for Bcl-xL in synaptic transmission. J Neurophysiol. 2008; 99:1515–1522. [PubMed: 18160428]
12. Alavian KN, et al. Bcl-xL regulates metabolic efficiency of neurons through interaction with the mitochondrial F1FO ATP synthase. Nat Cell Biol. 2011; 13:1224–1233. [PubMed: 21926988]
13. Verstreken P, et al. Synaptic mitochondria are critical for mobilization of reserve pool vesicles at Drosophila neuromuscular junctions. Neuron. 2005; 47:365–378. [PubMed: 16055061]
14. Blondeau F, et al. Tandem MS analysis of brain clathrin-coated vesicles reveals their critical involvement in synaptic vesicle recycling. Proc Natl Acad Sci U S A. 2004; 101:3833–3838. [PubMed: 15007177]
15. Dittman J, Ryan TA. Molecular circuitry of endocytosis at nerve terminals. Annual review of cell and developmental biology. 2009; 25:133–160.
16. Slepnev VI, Ochoa GC, Butler MH, Grabs D, De Camilli P. Role of phosphorylation in regulation of the assembly of endocytic coat complexes. Science. 1998; 281:821–824. [PubMed: 9694653]
17. Sakaba T, Neher E. Calmodulin mediates rapid recruitment of fast-releasing synaptic vesicles at a calyx-type synapse. Neuron. 2001; 32:1119–1131. [PubMed: 11754842]
18. Virmani T, Atasoy D, Kavalali ET. Synaptic vesicle recycling adapts to chronic changes in activity. J Neurosci. 2006; 26:2197–2206. [PubMed: 16495446]
19. Kidokoro Y, et al. Synaptic vesicle pools and plasticity of synaptic transmission at the Drosophila synapse. Brain Res Brain Res Rev. 2004; 47:18–32. [PubMed: 15572160]
20. Sara Y, Virmani T, Deak F, Liu X, Kavalali ET. An isolated pool of vesicles recycles at rest and drives spontaneous neurotransmission. Neuron. 2005; 45:563–573. see comment. [PubMed: 15721242]
21. Kuromi H, Kidokoro Y. Two distinct pools of synaptic vesicles in single presynaptic boutons in a temperature-sensitive Drosophila mutant, shibire. Neuron. 1998; 20:917–925. [PubMed: 9620696]
22. Kavalali ET. Multiple vesicle recycling pathways in central synapses and their impact on neurotransmission. The Journal of physiology. 2007; 585:669–679. [PubMed: 17690145]
23. Sun T, et al. The role of calcium/calmodulin-activated calcineurin in rapid and slow endocytosis at central synapses. J Neurosci. 2010; 30:11838–11847. [PubMed: 20810903]
24. Wu XS, et al. Ca(2+) and calmodulin initiate all forms of endocytosis during depolarization at a nerve terminal. Nat Neurosci. 2009; 12:1003–1010. [PubMed: 19633667]
25. Ryan TA, Smith SJ. Vesicle pool mobilization during action potential firing at hippocampal synapses. Neuron. 1995; 14:983–989. [PubMed: 7748565]
26. Burrone J, Li Z, Murthy VN. Studying vesicle cycling in presynaptic terminals using the genetically encoded probe synaptopHluorin. Nat Protoc. 2006; 1:2970–2978. [PubMed: 17406557]
27. Fernandez-Alfonso T, Ryan TA. The kinetics of synaptic vesicle pool depletion at CNS synaptic terminals. Neuron. 2004; 41:943–953. [PubMed: 15046726]
28. Sankaranarayanan S, De Angelis D, Rothman JE, Ryan TA. The use of pHluorins for optical measurements of presynaptic activity. Biophys J. 2000; 79:2199–2208. [PubMed: 11023924]
29. Miesenbock G, De Angelis DA, Rothman JE. Visualizing secretion and synaptic transmission with pH-sensitive green fluorescent proteins. Nature. 1998; 394:192–195. [PubMed: 9671304]
30. Oltersdorf T, et al. An inhibitor of Bcl-2 family proteins induces regression of solid tumours. Nature. 2005; 435:677–681. [PubMed: 15902208]
31. Alavian L, Collis Bonanni, Zeng Sacchetti, Lazrove Nabili, Flaherty Graham, Chen Messerli, Mariggio Rahner, McNay Shore, Smith Hardwick. Jonas Bcl-x(L) regulates metabolic efficiency of neurons through interaction with the mitochondrial F(1)F(O) ATP synthase. Nat Cell Biol. 2011; 13:1224–1233. [PubMed: 21926988]
32. Chen YB, Aon MA, Hsu YT, Soane L, Teng X, McCaffery JM, Cheng WC, Qi B, Li H, Alavian KN, Dayhoff-Brannigan M, Zou S, Pineda FJ, O'Rourke B, Ko YH, Pedersen PL, Kaczmarek LK, Jonas EA, Hardwick JM. Bcl-xL regulates mitochondrial energetics by stabilizing the inner membrane potential. J Cell Biol. 2011; 195:263–276. [PubMed: 21987637]
33. Galluzzi L, Blomgren K, Kroemer G. Mitochondrial membrane permeabilization in neuronal injury. Nat Rev Neurosci. 2009; 10:481–494. [PubMed: 19543220]

34. Kaufmann T, et al. Characterization of the signal that directs Bcl-x(L), but not Bcl-2, to the mitochondrial outer membrane. J Cell Biol. 2003; 160:53–64. [PubMed: 12515824]
35. Kluck RM, Bossy-Wetzel E, Green DR, Newmeyer DD. The release of cytochrome c from mitochondria: a primary site for Bcl-2 regulation of apoptosis. Science. 1997; 275:1132–1136. see comment. [PubMed: 9027315]
36. Hsu YT, Wolter KG, Youle RJ. Cytosol-to-membrane redistribution of Bax and Bcl-X(L) during apoptosis. Proc Natl Acad Sci U S A. 1997; 94:3668–3672. [PubMed: 9108035]
37. Berman SB, et al. Bcl-x L increases mitochondrial fission, fusion, and biomass in neurons. J Cell Biol. 2009; 184:707–719. [PubMed: 19255249]
38. Bossy-Wetzel E, Barsoum MJ, Godzik A, Schwarzenbacher R, Lipton SA. Mitochondrial fission in apoptosis, neurodegeneration and aging. Current Opinion in Cell Biology. 2003; 15:706–716. [PubMed: 14644195]
39. Karbowski M, et al. Spatial and temporal association of Bax with mitochondrial fission sites, Drp1, and Mfn2 during apoptosis. J Cell Biol. 2002; 159:931–938. [PubMed: 12499352]
40. Karbowski M, Youle RJ. Dynamics of mitochondrial morphology in healthy cells and during apoptosis. Cell Death Differ. 2003; 10:870–880. [PubMed: 12867994]
41. Shaw JM, Nunnari J. Mitochondrial dynamics and division in budding yeast. Trends in Cell Biology. 2002; 12:178–184. [PubMed: 11978537]
42. Karbowski M, Neutzner A, Youle RJ. The mitochondrial E3 ubiquitin ligase MARCH5 is required for Drp1 dependent mitochondrial division. J Cell Biol. 2007; 178:71–84. [PubMed: 17606867]
43. Uo T, et al. Drp1 levels constitutively regulate mitochondrial dynamics and cell survival in cortical neurons. Exp Neurol. 2009; 218:274–285. [PubMed: 19445933]
44. Otera H, et al. Mff is an essential factor for mitochondrial recruitment of Drp1 during mitochondrial fission in mammalian cells. J Cell Biol. 2010; 191:1141–1158. [PubMed: 21149567]
45. Lenzi D, Crum J, Ellisman MH, Roberts WM. Depolarization redistributes synaptic membrane and creates a gradient of vesicles on the synaptic body at a ribbon synapse. Neuron. 2002; 36:649–659. [PubMed: 12441054]
46. Lu Y, Rolland SG, Conradt B. A molecular switch that governs mitochondrial fusion and fission mediated by the BCL2-like protein CED-9 of Caenorhabditis elegans. Proc Natl Acad Sci U S A. 2011; 108:E813–822. [PubMed: 21949250]
47. Sakaba T, Neher E. Calmodulin mediates rapid recruitment of fast-releasing synaptic vesicles at a calyx-type synapse. Neuron. 2001; 32:1119–1131. see comment. [PubMed: 11754842]
48. Li Z, Okamoto K, Hayashi Y, Sheng M. The importance of dendritic mitochondria in the morphogenesis and plasticity of spines and synapses. Cell. 2004; 119:873–887. see comment. [PubMed: 15607982]
49. Pang ZP, Cao P, Xu W, Sudhof TC. Calmodulin controls synaptic strength via presynaptic activation of calmodulin kinase II. J Neurosci. 30:4132–4142. [PubMed: 20237283]
50. Rostovtseva TK, et al. Bax activates endophilin B1 oligomerization and lipid membrane vesiculation. J Biol Chem. 2009; 284:34390–34399. [PubMed: 19805544]
51. Jonas EA, et al. Proapoptotic N-truncated BCL-xL protein activates endogenous mitochondrial channels in living synaptic terminals. Proc Natl Acad Sci U S A. 2004; 101:13590–13595. [PubMed: 15342906]
52. Basanez G, et al. Bax-type apoptotic proteins porate pure lipid bilayers through a mechanism sensitive to intrinsic monolayer curvature. J Biol Chem. 2002; 277:49360–49365. [PubMed: 12381734]
53. Basanez G, et al. Pro-apoptotic cleavage products of Bcl-xL form cytochrome c-conducting pores in pure lipid membranes. J Biol Chem. 2001; 276:31083–31091. [PubMed: 11399768]
54. Karbowski M, Jeong SY, Youle RJ. Endophilin B1 is required for the maintenance of mitochondrial morphology. J Cell Biol. 2004; 166:1027–1039. [PubMed: 15452144]
55. Farsad K, et al. Generation of high curvature membranes mediated by direct endophilin bilayer interactions. J Cell Biol. 2001; 155:193–200. [PubMed: 11604418]

56. Ringstad N, et al. Endophilin/SH3p4 is required for the transition from early to late stages in clathrin-mediated synaptic vesicle endocytosis. Neuron. 1999; 24:143–154. [PubMed: 10677033]
57. Schuske KR, et al. Endophilin is required for synaptic vesicle endocytosis by localizing synaptojanin. Neuron. 2003; 40:749–762. [PubMed: 14622579]
58. Milosevic I, et al. Recruitment of endophilin to clathrin-coated pit necks is required for efficient vesicle uncoating after fission. Neuron. 2011; 72:587–601. [PubMed: 22099461]
59. Morgan JR, Augustine GJ, Lafer EM. Synaptic vesicle endocytosis: the races, places, and molecular faces. Neuromolecular medicine. 2002; 2:101–114. [PubMed: 12428806]
60. Guo X, et al. The GTPase dMiro is required for axonal transport of mitochondria to Drosophila synapses. Neuron. 2005; 47:379–393. [PubMed: 16055062]
61. Krueger SR, Kolar A, Fitzsimonds RM. The presynaptic release apparatus is functional in the absence of dendritic contact and highly mobile within isolated axons. Neuron. 2003; 40:945–957. [PubMed: 14659093]
62. Brewer GJ. Isolation and culture of adult rat hippocampal neurons. J Neurosci Methods. 1997; 71:143–155. [PubMed: 9128149]
63. Lois C, Hong EJ, Pease S, Brown EJ, Baltimore D. Germline transmission and tissue-specific expression of transgenes delivered by lentiviral vectors. Science. 2002; 295:868–872. [PubMed: 11786607]
64. Allen TG. Preparation and maintenance of single-cell micro-island cultures of basal forebrain neurons. Nat. protoc. 2006; 1:2543–2550. [PubMed: 17406501]
65. Komai S, et al. Postsynaptic excitability is necessary for strengthening of cortical sensory responses during experience-dependent development. Nat Neurosci. 2006; 9:1125–1133. [PubMed: 16921372]
66. Tokuyasu KT. A technique for ultracryotomy of cell suspensions and tissues. J Cell Biol. 1973; 57:551–565. [PubMed: 4121290]

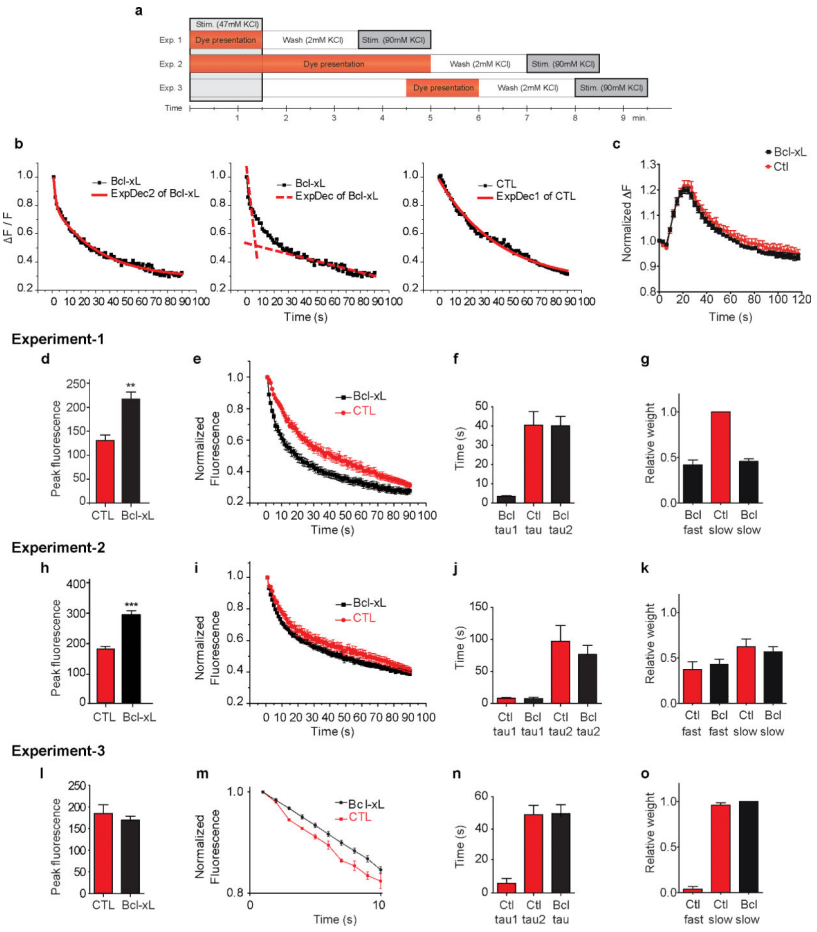

Fig. 1. Bcl-x_L over-expression enhances the rate of release of styryl dyes in hippocampal neurons

a. Diagram of protocols for experiments (1-3) described in text.

b. Examples of exponential fits to normalized fluorescence change of FM 5-95 puncta during stimulation with 90 mM KCl. Left panel: Bi-exponential fit to normalized fluorescence change from cells over-expressing Bcl-x_L (ExpDec2 of Bcl-x_L=bi-exponential decay of fluorescence). Center panel: Dotted lines model two different exponents of left panel (ExpDec of Bcl-x_L=bi-exponential fit to fluorescence decay shown as one dotted line for each exponent). Right panel: Single exponential fit to the normalized fluorescence change from a GFP control neuron (ExpDec1 of control=single exponential decay of fluorescence).

c. Time course of normalized fluorescence of 5 μM Fluo-4 measured in synaptic boutons during electrical stimulation (100 action potentials at 10 Hz; n=15 DsRed expressing cells, n=15 DsRed-Bcl-x_L expressing cells).

d. Peak fluorescence after loading with Exp 1 protocol (prior to unloading) of individual FM 5-95 puncta (n=10 GFP CTL puncta, 14 GFP- Bcl-x_L puncta; **$p < 0.0013$; three independent cultures). In all experiments, Bcl-x_L expressing and GFP-expressing controls are pairs from the same culture.

e. Normalized fluorescence change in 90 mM KCl (n=10 GFP CTL puncta, 14 GFP- Bcl-x_L puncta).

f. Time constants for exponential fits to all experiments in e.

g. Relative weights of exponential pools for experiments in e.
h. Peak fluorescence of FM 5-95 puncta (protocol for Exp 2); n=14 GFP CTL puncta, 15 GFP-Bcl-x_L puncta; three independent cultures; ***$p < 0.0001$).
i. Normalized fluorescence change in 90 mM KCl (Exp 2 protocol; n=14 GFP CTL puncta, 15 GFP-Bcl-x_L puncta).
j. Time constants for exponential fits to experiments in i.
k. Relative weights of exponential pools for experiments in i.
l. Peak fluorescence of FM 5-95 puncta (Exp 3 protocol; n=11 GFP CTL puncta, 20 GFP-Bcl-x_L puncta; three independent cultures).
m. Normalized fluorescence change in 90 mM KCl (Exp 3 protocol; n=5 GFP CTL puncta, 10 GFP-Bcl-x_L puncta). The initial 10 s of fluorescence decline is shown. 5 CTL puncta are represented to emphasize the bi-exponential effect found in a subgroup of CTL puncta. No punctal fluorescence changes from GFP-Bcl-x_L expressing cells required bi-exponential fits.
n. Time constants for exponential fits to experiments such as in m (n=9 GFP CTL puncta, n=10 GFP-Bcl-x_L puncta).
o. Relative weights of exponential pools for experiments in m. Statistics are represented as mean +/- S.E.M.

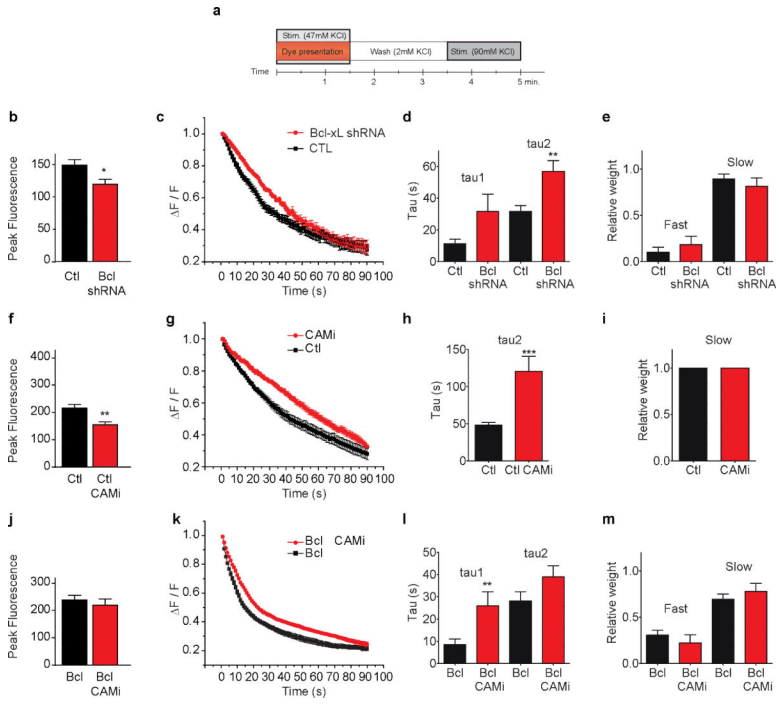

Fig. 2. Endogenous Bcl-x_L participates in normal vesicle pool dynamics

a. Diagram of protocol 1 for all experiments in Figure 2.

b. Peak fluorescence of FM 5-95 puncta (n=13 scrambled shRNA, 10 Bcl-x_L shRNA; *p<0.03; puncta from 5 different cells, three independent cultures).

c. Normalized fluorescence in 90 mM KCl (n=9 scrambled shRNA, n=7 Bcl-x_L shRNA; 5 different cells, three independent cultures.

d. Time constants for exponential fits to experiments in c (n=12 scrambled shRNA, n=7 Bcl-x_L shRNA ***p< 0.0001 comparing tau 2 for the two conditions).

e. Relative weights of two exponential pools for experiments in c.

f. Peak fluorescence of FM 5-95 in CTL and CaMi-treated cells (n=10 puncta each; **p<0.003; 5 different cells each from three independent cultures). Cells were exposed to 30 μM CaMi or vehicle for 30 min. prior to loading with FM 5-95.

g. Normalized fluorescence in 90 mM KCl (n=10 CTL, n=8 puncta of CaMi-treated cells; 5 different cells for each condition from three independent cultures).

h. Time constants for exponential fits to experiments in g (***p=0.0009).

i. Relative weights of exponential pools for experiments in g.

j. Peak fluorescence of FM 5-95 puncta in GFP-Bcl-x_L expressing cells and GFP-Bcl-x_L expressing cells treated with CaMi (n=8 each; 3 different coverslips in each condition).

k. Normalized fluorescence in 90 mM KCl (n=7 GFP- Bcl-x_L and 8 GFP- Bcl-x_L + CaMi puncta; 3 different cells for each condition).

l. Time constants for exponential fits to experiments in k (n=12 GFP- Bcl-x_L and 7 GFP-Bcl-x_L + CaMi puncta; **p=0.0069, comparing tau 1 for the two conditions).

m. Relative weights of exponential pools for experiments in k. Statistics are represented as mean +/- S.E.M.

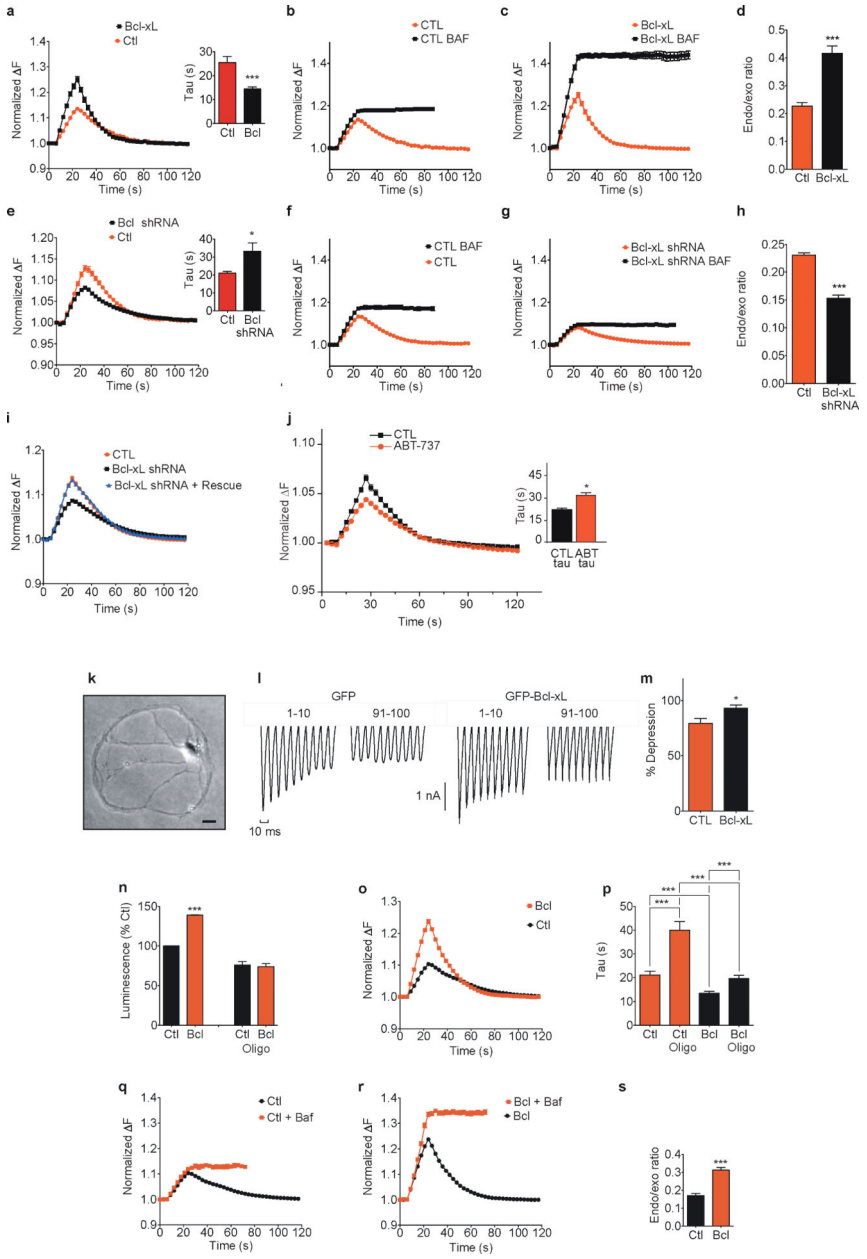

Fig 3. Bcl-x_L increases the rate of mitochondrial ATP-resistant early endocytosis

a. Normalized fluorescence change of synaptopHluorin puncta before, during and after electrical stimulation (with 100 action potentials, 10 Hz; n=15 puncta from DsRed-Bcl-x_L cells, n=15 mito-RFP CTL). Inset: time constants of change in fluorescence after stimulation (***p=0.0002; 3 independent cultures. Experiment repeated with 8 different cultures.

b. Normalized fluorescence (n=15 DsRed control puncta before and after 5 μM bafilomycin). Non-normalized data: Suppl. Fig. 5a.

c. Normalized fluorescence (n=15 DsRed Bcl-x_L puncta before and after bafilomycin).

d. Ratio of difference in peak fluorescence before and after bafilomycin to peak in bafilomycin of traces in b and c (***p< 0.0001).

e. Normalized fluorescence (n=15 puncta from each DsRed-Bcl-x_L shRNA or DsRed (CTL) cells). Inset: time course of change in fluorescence after stimulation (n=15 puncta each group; *p=0.0203; 3 independent cultures).

f. Normalized fluorescence (n=15 puncta from DsRed controls before and after bafilomycin).

g. Normalized fluorescence (n=15 puncta from DsRed Bcl-x_L shRNA before and after bafilomycin).

h. Ratio of difference in peak fluorescence before and after bafilomycin over peak in bafilomycin of traces in f and g (***p< 0.0001).

i. Normalized fluorescence (n=15 puncta from DsRed control or DsRed Bcl-x_L shRNA, or both DsRed Bcl-x_L shRNA plus shRNA-resistant Bcl-x_L; 3 independent coverslips in each group.

j. Normalized fluorescence for vehicle or 5 min. after exposure to 10 μM ABT-737; N=6). Inset: time constants of fluorescence changes (*p<0.02).

k. Phase image of single autaptic hippocampal neuron in culture DIV 16. Scale bar= 20 μm.

l. Synaptic depression of GFP-Bcl-x_L or control GFP (10 Hz stimulation, first and last 10 of 100 synaptic responses).

m. Summary data of percentage change in average amplitude of last 10 compared to first 10 synaptic responses (n=8 control GFP and 9 GFP-Bcl-x_L cells, two independent cultures; *p = 0.017).

n. ATP levels (luciferin/luciferase) of lysed neurons expressing the indicated constructs; oligomycin=5 μg/ml for 5 min; n=12 wells each group,*** p<0.0001).

o. Normalized fluorescence in 5 μg/ml oligomycin (stimulation 5 min. after oligomycin application n=10 puncta each from DsRed-Bcl-x_L or mito-RFP (CTL) expressing cells).

p. Time constants of change in fluorescence after stimulation for data in o (n=10 each for oligomycin; ***p<0.0001 comparing Bcl-x_L to control; non-oligomycin puncta n=37 for each condition, ***p<0.0001 comparing Bcl-x_L to control; oligomycin CTL data compared to non-oligo control data; ***p<0.0001; Bcl-x_L oligomycin-treated compared to non-oligomycin ***p=0.0005).

q. Normalized fluorescence before and after 5 μM bafilomycin in oligomycin-treated cells (n=10 puncta, three independent cover slips; mito-RFP controls).

r. Normalized fluorescence before and after 5 μM bafilomycin (n=10 puncta, three independent cover slips, DsRed-Bcl-x_L).

s. Ratio of difference in peak fluorescence before and after bafilomycin over peak in bafilomycin of traces shown in q and r (***p< 0.0001). Statistics are represented as mean +/- S.E.M.

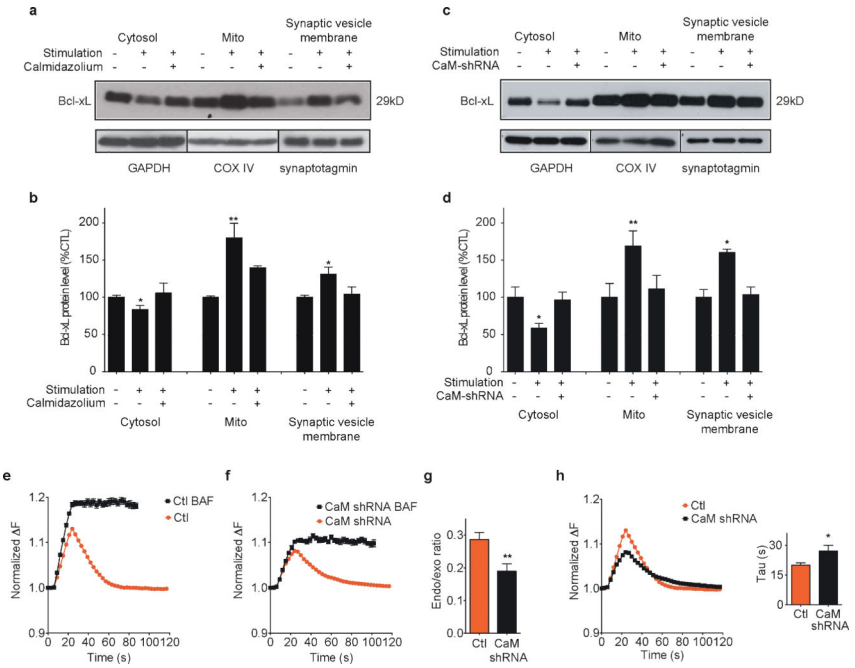

Fig. 4. Calmodulin-dependent Bcl-x_L translocation to synaptic vesicle membranes in stimulated neurons

a. Immunoblots for Bcl-x_L of indicated sub-fractions of cell lysates of cultured unstimulated hippocampal neurons or stimulated with 90 mM KCl for 90 s with or without CaMi. GAPDH serves as protein control for cytosolic protein amount, COX IV as control for mitochondrial protein amount, synaptotagmin as control for synaptic vesicle membrane protein amount.

b. Group data for protein densities for all experiments in a (n=3 blots; *$p < 0.03$, one-tailed unpaired student's t test of protein amount after stimulation compared to before stimulation; **$p < 0.009$, one-tailed unpaired student's t test of protein amount after stimulation compared to before stimulation).

c. Immunoblots for Bcl-x_L of indicated sub-fractions of cell lysates of cultured unstimulated or stimulated neurons. The right lane of each cell subfraction indicates level of Bcl-x_L from cells transduced with DsRed calmodulin shRNA. GAPDH serves as protein control for cytosolic protein amount, COX IV as control for mitochondrial protein amount, synaptotagmin as control for synaptic vesicle membrane protein amount.

d. Group data for protein densities for all experiments in c (n=3 blots; *$p < 0.03$, **$p=0.0081$ one-tailed unpaired student's t test of protein amount after stimulation compared to before stimulation).

e. Normalized (to starting value) fluorescence change of synaptopHluorin puncta before, during and after electrical stimulation (with 100 action potentials, 10 Hz; n=10 puncta from DsRed expressing cells before and after 5 μM bafilomycin).

f. Normalized fluorescence change (n=10 puncta from DsRed CaM shRNA expressing cells before and after bafilomycin.

g. Ratio of difference in peak fluorescence change before and after bafilomycin to the peak fluorescence in bafilomycin of traces shown in e and f (**$p=0.006$).

h. Normalized fluorescence change (n=10 puncta for calmodulin shRNA or scrambled shRNA; 3 cells each, one culture). Inset: bar graphs of time constants of fluorescence changes (*p=0.038). Statistics are represented as mean +/- S.E.M.

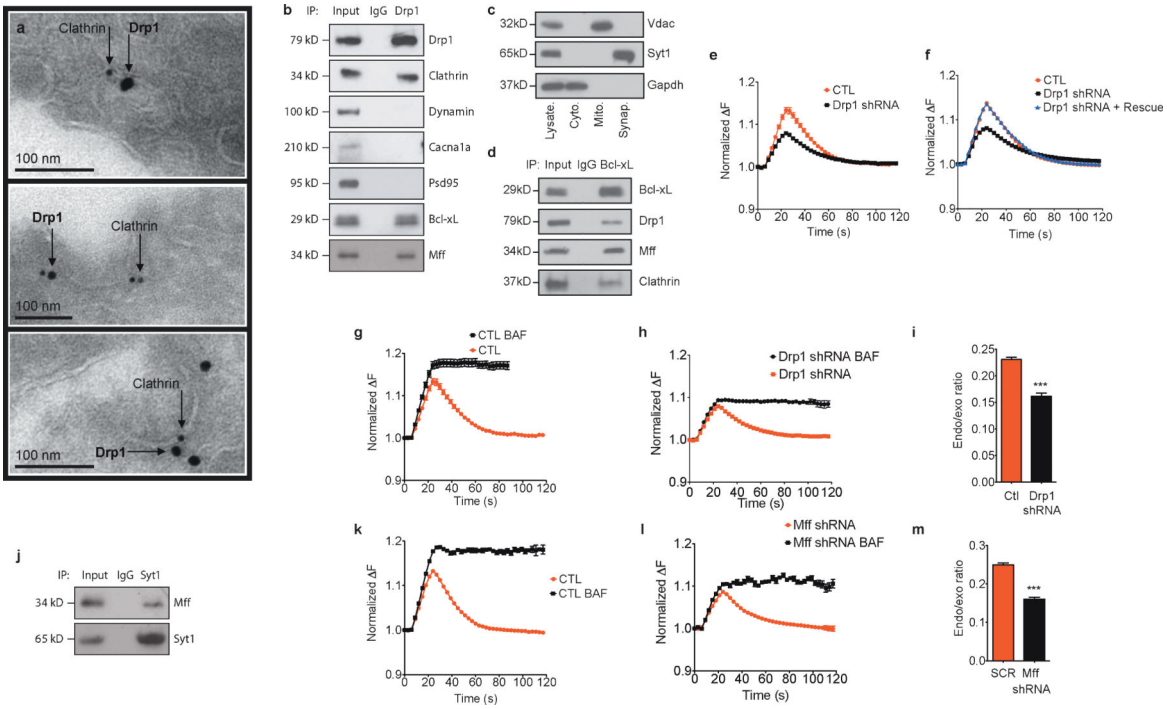

Fig. 5. Drp1 is co-localized with clathrin and Mff on synaptic vesicles

a. Immuno-electron micrographs of Drp1 on clathrin-coated pits. Cultured hippocampal neurons were stimulated with 90 mM KCl for 90 s prior to fixation for electron microscopy (EM).

b. Co-immunoprecipitation of whole rat brain lysate using indicated antibodies (IP refers to antibodies used for immunoprecipitation. Titles at right of blot refer to antibodies used for immunoblotting. Left lane represents cell lysate).

c. Immunoblots of subcellular fractions (as indicated) of rat brain lysate using the indicated antibodies. Left lane shows cell lysate.

d. Co-immunoprecipitation of purified synaptic vesicle fraction using the indicated antibodies (left lane represents cell lysate).

e. Normalized fluorescence change before, during and after electrical stimulation (n=15 puncta from DsRed controls or DsRed Drp1 shRNA; 3 independent cultures each group.

f. Normalized fluorescence change (n=15 puncta each DsRed control (red trace, same control data as for Bcl-x_L shRNA in 3i), DsRed Drp1 shRNA expressing cells (black trace), or from cells expressing both DsRed Drp1shRNA plus Drp1 shRNA-resistant Drp1 overexpressing construct (blue trace). 3 independent cultures).

g. Normalized fluorescence change (n=15 puncta from DsRed control expressing cells before and after bafilomycin). These control data are the same as the DsRed control data in Fig. 3f but are provided here for comparison to 5h.

h. Normalized fluorescence change (n=15 puncta from DsRed Drp1 shRNA expressing cells before and after bafilomycin).

i. Peak fluorescence change ratios of traces shown in g and h (***p< 0.0001).

j. Co-immunoprecipitation of whole rat brain lysate using indicated antibodies (IP refers to antibodies used for immunoprecipitation; Titles at right of blot refers to antibodies used for immunoblotting. Left lane represents cell lysate).

k. Normalized fluorescence change; n=12 puncta from scrambled shRNA expressing cells before and after 5 μM bafilomycin, 12 different coverslips, 2 independent cultures.

l. Normalized fluorescence change; n=12 puncta from Mff shRNA expressing cells before and after bafilomycin, 13 different coverslips, 2 independent cultures.

m. Peak fluorescence change ratios of traces shown in k and l (***$p < 0.0001$). Statistics are represented as mean +/- S.E.M.

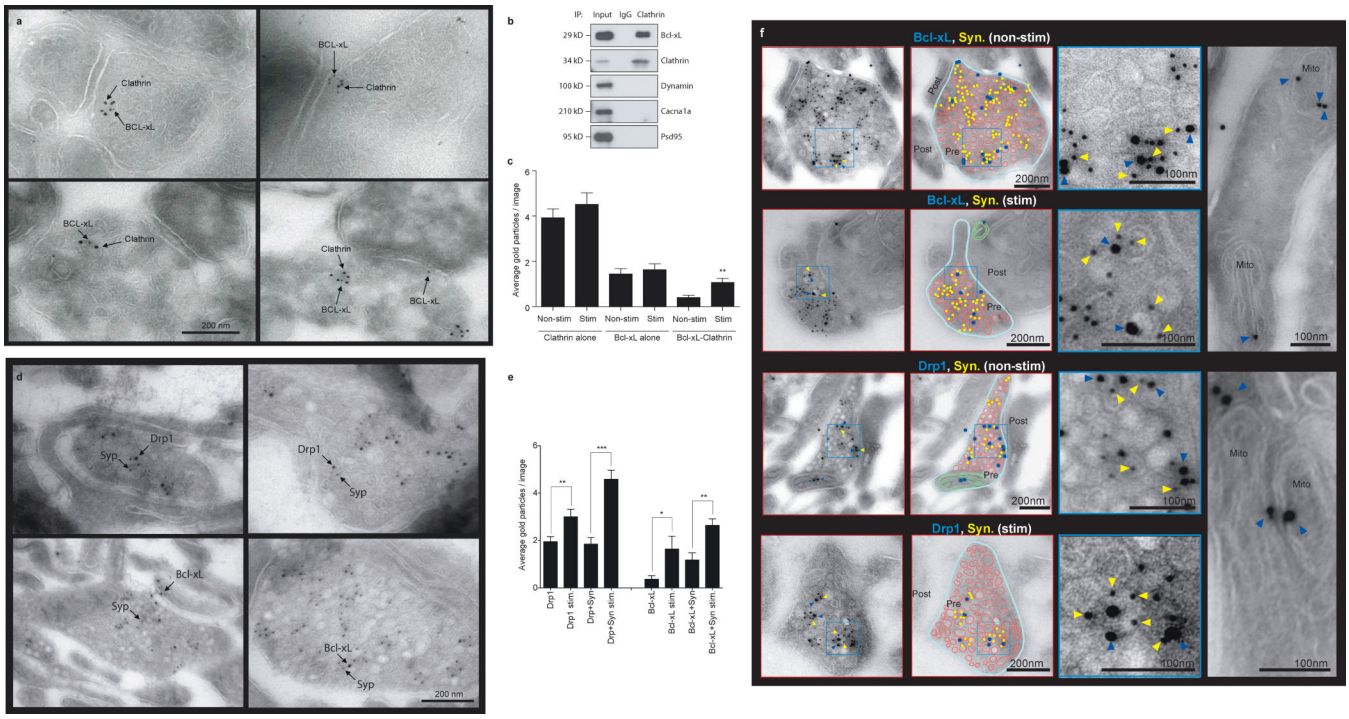

Fig. 6. Bcl-x_L and Drp1 co-localize with synaptophysin on synaptic vesicles

a. Immuno-electron micrographs co-localizing clathrin and Bcl-x_L. Cultured hippocampal neurons were stimulated with 90 mM KCl for 90 s just prior to fixation for EM.

b. Co-immunoprecipitation using indicated antibodies (IP refers to antibody used for immunoprecipitation; antibodies used for immunoblotting are labeled at right). Left lane represents cell lysate.

c. Average number of gold particles in electron micrographs of synapses. n=25 micrographs of non-stimulated cells, n=27 micrographs of stimulated cells. First two histograms represent clathrin-labeled particles, second two histograms represent Bcl-x_L-labeled particles, third set of histograms represents co-localizing Bcl-x_L- and clathrin-labeled particles on the same synaptic vesicle (p=0.0014).

d. (Top) Immuno-electron micrographs showing co-localization of Drp1 and synaptophysin in unstimulated (left panel) and stimulated synapses (right panel). (Bottom) Immuno-electron micrographs showing co-localization of Bcl-x_L and synaptophysin in unstimulated (left panel) and stimulated synapses (right panel).

e. Average number of gold particles in electron micrographs of synapses treated with antibodies and stimulation as labeled (left to right: n=20, 17, 20, 17, 11, 11, 11, 11; **p=0.0081 (Drp1 nonstim. vs. Drp1 stim.). ***p<0.0001 (co-localization of Drp1 and synaptophysin non-stim. vs. stim.). *p=0.0356 (Bcl-x_L non-stim. vs. Bcl-x_L stim.). **p=0.0019 (co-localization of Bcl-x_L and synaptophysin non-stim. vs. stim.).

f. (Left top) Immuno-electron micrographs showing co-localization of Bcl-x_L (10 nm gold balls) and synaptophysin (5 nm gold balls). (Left bottom) Immuno-electron micrographs showing co-localization of Drp1 (10 nm gold balls) and synaptophysin (5 nm gold balls). In the schematic diagrams to the right of, and superimposed on, the images, the presynaptic membrane is colored in light blue, synaptic vesicles are colored in red, gold balls indicating

Bcl-x_L or Drp1 antibody labeling are colored in dark blue, gold balls indicating synaptophysin antibody labeling are colored in yellow, green indicates mitochondria. Enlarged insets show synaptophysin, Drp1 and Bcl-x_L immunolabeling (yellow arrows indicate synaptophysin antibody labeling, blue arrows indicate Bcl-x_L (top two images) or Drp1 (bottom two images). The right-most panels picture mitochondria (top shows Bcl-x_L immunolabeling, bottom shows Drp1 immunolabeling. Statistics are represented as mean +/- S.E.M.

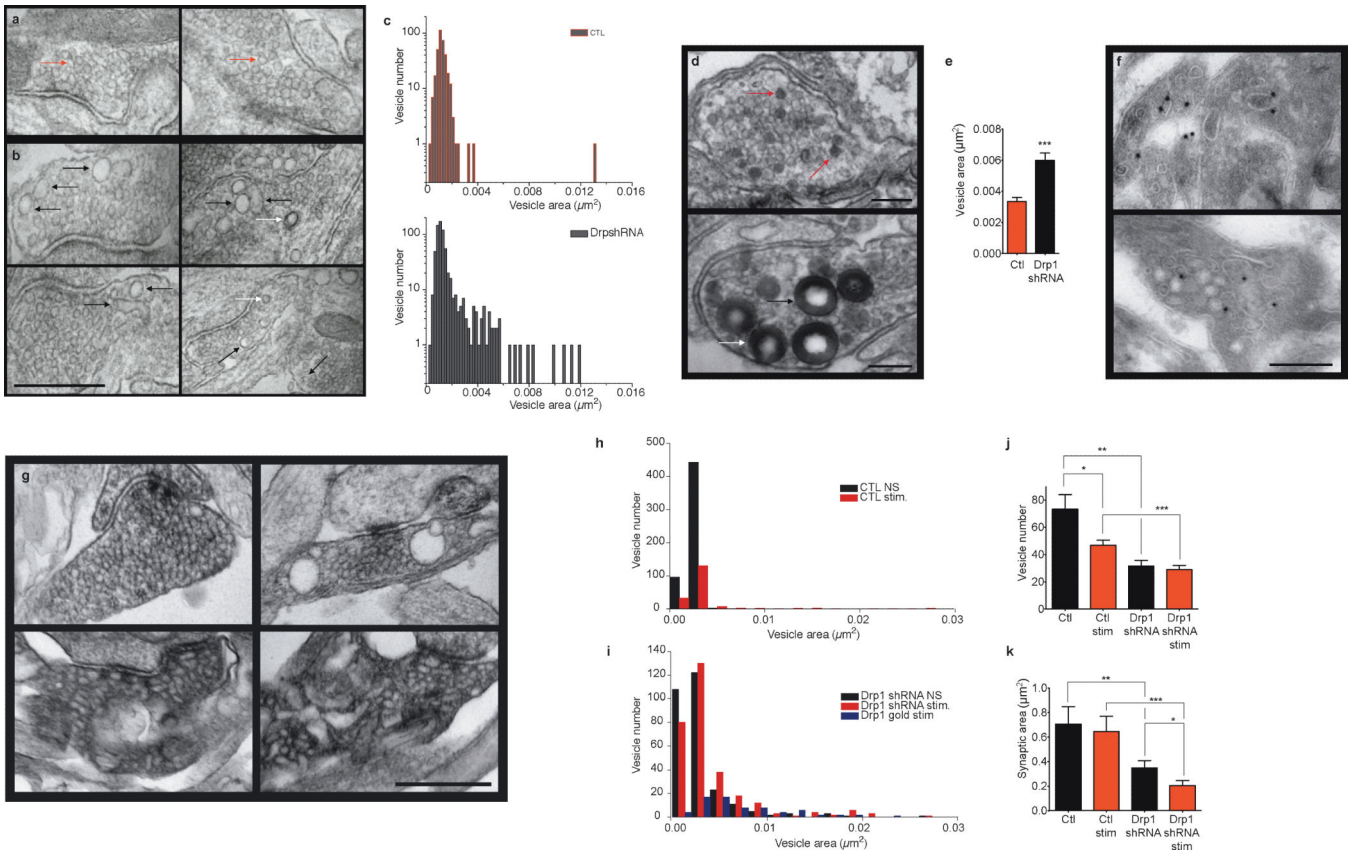

Fig. 7. Drp1 is required for formation of normal endocytotic vesicles

a. Electron micrographs of resting synapses of hippocampal neurons transduced with scrambled GFP-shRNA. Red arrows demonstrate representative control synaptic vesicles. Scale bar is shown in 7b.

b. Electron micrographs of resting synapses of hippocampal neurons transduced with GFP-Drp1 shRNA. Black arrows indicate enlarged vesicles and (in lower right hand panel) a vesicle with an elongated neck. White arrows indicate clathrin-coated pits, which tend to be more frequently seen in micrographs of synapses of Drp1 shRNA expressing neurons. Scale bar = 500 nm.

c. Histograms of all vesicle area measurements (n=6 micrographs of scrambled shRNA expressing neurons, 347 vesicles; n=8 micrographs of Drp1 shRNA expressing neurons, 667 vesicles.

d. Electron micrographs of stimulated synapses of hippocampal neurons transduced with scrambled GFP shRNA (top image) or with GFP Drp1 shRNA (bottom image); blots were fixed just after stimulation with 90 mM KCl in the presence of horse radish peroxidase (HRP). Scale bar = 200 nm. Red arrows demonstrate HRP-labeled vesicles in controls, black arrows demonstrate HRP-labeled vesicles in Drp1 shRNA. White arrow shows an endocytotic pit pinching off the plasma membrane.

e. Quantification of area (μm^2) of all HRP-labeled vesicles (n=9 images, 98 total vesicles for control; n=11 images, 127 total vesicles for Drp1 shRNA, ***p<0.0001).

f. Cryo-electron micrographs immuno-labeled with gold-tagged anti-VAMP antibodies after stimulation. Scale bar = 200 nm.

g. Electron micrographs of synapses of hippocampal neurons transduced with scrambled GFP shRNA (top images) or with GFP Drp1 shRNA (bottom images). Left panels represent unstimulated synapses, right panels represent stimulated synapses. Scale bar = 500 nm.

h-i. Histograms of all vesicle area measurements (μm^2) from panels in f, g (n=8 micrographs of control scrambled shRNA unstimulated synapses, n=5 micrographs of control scrambled shRNA stimulated synapses, n=9 micrographs of Drp1 shRNA unstimulated synapses, n=12 micrographs of Drp1 shRNA stimulated synapses, n=19 micrographs of Drp1 shRNA synapses immunogold labeled with anti-VAMP antibodies).

j. Quantification of number of vesicles in synapses such as shown in g (n=9 micrographs (synapses) each for unstimulated and stimulated scrambled shRNA, 9 micrographs for unstimulated Drp1 shRNA, 11 micrographs for stimulated Drp1 shRNA; *p = 0.0306, **p = 0.002, ***p<0.0001).

k. Quantification of synapse area (μm^2) of all synapses measured in j (*p=0.043; **p=0.007, ***p<0.0001). Statistics are represented as mean +/- S.E.M.

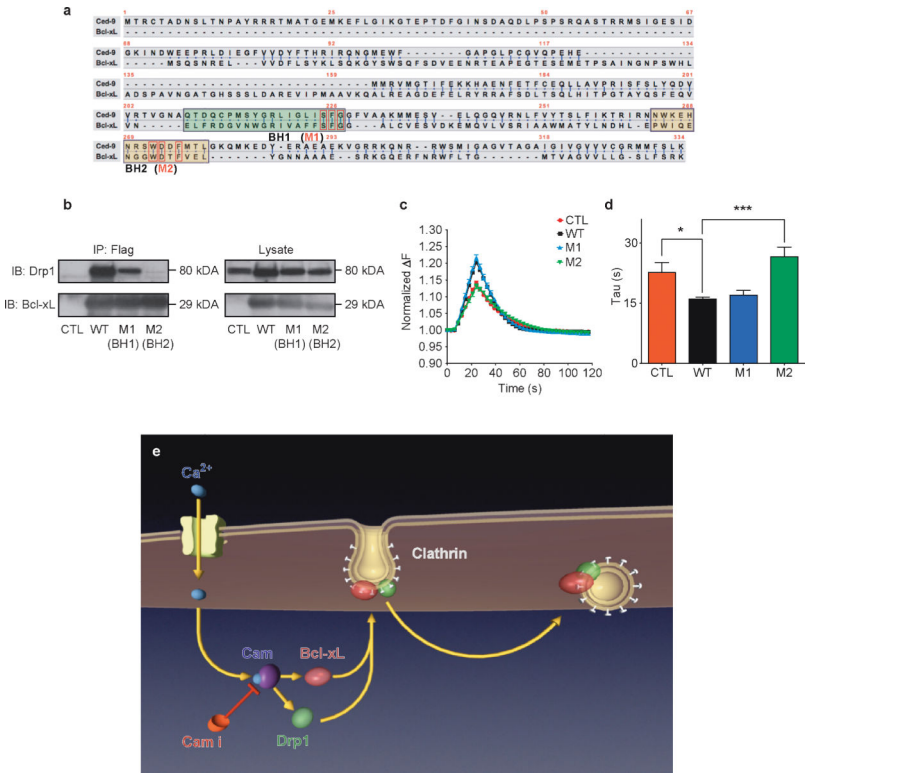

Figure 8. Mutations in BH2 domain of Bcl-x_L disrupt physical and functional interaction with Drp1

a. CED-9 and Bcl-x_L protein sequences. Green and yellow boxes specify BH1 and BH2 domains, respectively. Red boxes denote conserved mutated amino acids within each domain.

b. Immunoprecipitation by an anti-FLAG antibody of the wild type and mutant (M1 and M2) FLAG-tagged Bcl-x_L proteins. Samples were immunoblotted for Drp1 and Bcl-x_L. Lysate studies are shown in the right panel.

c. Normalized (to starting value) fluorescence change of synaptopHluorin puncta in hippocampal neurons expressing indicated constructs before, during and after electrical stimulation (with 100 action potentials, 10 Hz), n=10 puncta each from 3 cells each from one culture.

d. Group data for all experiments shown in c (*p=0.0169; ***p=0.0004).

e. Model showing order of events: 1) Neuronal stimulation leads to calcium influx. 2) Calcium binds to and activates Calmodulin (CaM), which is inhibited by calmidazolium (CaMi). 3) CaM causes the translocation of Bcl-x_L and Drp1 to clathrin-coated pits where Bcl-x_L binds to and activates Drp1. 4) Drp1 is in part responsible for the formation of normally curved endocytotic vesicles. Knock down or functional inhibition of Bcl-x_L, Drp1 or CaM disrupts this process, slowing endocytosis.